

Part V
Oncology

Chapter 21

Back to the Future: Nuclear Medicine Rediscovered Its Therapeutic Roots

Rodney J. Hicks

Abstract Before the advent of diagnostic imaging, nuclear medicine was a treatment modality. The first therapeutic application of radioisotopes was almost contemporaneous with the discovery of radioactivity. P-32 became one of the first effective therapies for a range of malignant blood disorders; I-131 was established as the benchmark for the treatment of metastatic thyroid cancer; Sr-89 was recognised to provide palliative benefit in advanced prostate cancer. The development of tomographic imaging with SPECT and PET, further enhanced by hybrid CT or MRI devices, has recently focussed the speciality of nuclear medicine on the diagnostic use of isotopes. Against this trend there has been renewed awareness on the ability of radiotracers to identify potential therapeutic targets and to use this information to select patients for and to monitor the efficacy of targeted therapies using radioisotopes. This process has been termed “theranostics”. A significant factor in the rebirth of therapeutic nuclear medicine has been the development of peptides labelled with Ga-68 and Lu-177. Ga-68 DOTA-octreotate PET/CT and Lu-177 DOTA-octreotate peptide receptor radionuclide therapy (PRRT) provides the modern prototype of the theranostic paradigm. Experience with PRRT has, however, emphasised the need for a more rigorous scientific approach to radionuclide therapy. The future holds promise of wide range of therapeutic options based on diagnostic/therapeutic pairs including I-124/I-131 and Cu-64/Cu-67. Quantitative SPECT/CT and PET/CT will be key platform technologies for planning and monitoring such therapy and will realise the true promise of molecular imaging in characterising rather than just finding disease.

R.J. Hicks, MB BS (Hons), MD, FRACP (✉)

Cancer Imaging, The Peter MacCallum Cancer Centre, St Andrew’s Place East, Melbourne, VIC 3002, Australia

Neuroendocrine Service, The Peter MacCallum Cancer Centre, Melbourne, Australia

Department of Medicine, St Vincent’s Hospital, Fitzroy, VIC, Australia

Department of Radiology, Royal Melbourne Hospital, Parkville, VIC, Australia

Molecular Imaging and Targeted Therapeutics Laboratory, The Sir Peter MacCallum

Department of Oncology, The University of Melbourne, Parkville, Australia

e-mail: rod.hicks@petermac.org

© The Author(s) 2016

Y. Kuge et al. (eds.), *Perspectives on Nuclear Medicine for Molecular Diagnosis and Integrated Therapy*, DOI 10.1007/978-4-431-55894-1_21

277

Keywords Positron emission tomography • Radionuclide therapy • Theranostics • Peptide receptor • Neuroendocrine tumour

21.1 Introduction

Many current practitioners working in nuclear medicine are unaware of its rich history as a therapeutic modality. For interested readers, a delightful series of anecdotes and historical vignettes are contained in Marshall Brucer's "A Chronology of Nuclear Medicine" (Publisher: Robert R Butaine (September 1990) ISBN-10: 096256740X, ISBN-13: 978-0962567407). To summarise this fascinating tale of discovery, serendipity and human sacrifice are beyond the scope of this paper but I will try to cover its key events in order to provide a background to current advances in nuclear medicine practice that I believe will be fundamental to its future evolution.

21.2 Radioisotopes Become Therapeutic Tools

Shortly after the discovery of radioactivity in naturally occurring elements by Henri Becquerel in 1896 and the subsequent isolation of radium by Marie and Pierre Curie in 1898, Pierre Curie became aware of the potential of radioactive elements to damage cells, when he himself sustained a very slow healing radiation ulcer on his chest after carrying a sample of radium to a lecture at the Sorbonne in Paris. Louis Pasteur opined that chance favours the prepared mind. In this case, this simultaneously unfortunate but fortuitous event led Pierre Curie to ponder whether radium might have potential therapeutic application in the treatment of malignant skin lesions. In a seminal example of translational research, he discussed this with a medical colleague, Henri-Alexandre Danlos, who successfully treated patients with aggressive squamous cell and basal cell cancers. This quickly led to the dissemination of radium throughout the world for treatment, first of skin cancers and, later, of all manner of malignancies. Intra-tumoural administration of radium was a forerunner of modern brachytherapy. However, it soon became clear that despite, at times, dramatic therapeutic effects, this treatment, particularly when administered systemically, could have significant side effects, including death but, particularly, haematological disorders and, in the case of radium, osteosarcoma. Marie Curie herself died of aplastic anaemia. Although this has been attributed to her exposure to radioisotopes, she also would have received substantial radiation while using unshielded X-rays while operating a field ambulance service in World War 1.

The development of the cyclotron by Ernest O. Lawrence provided a range of new isotopes [1]. One of these, P-32, was found to suppress blood counts, and again in a serendipitous manner, Lawrence's brother was a haematologist and decided to try this agent for the treatment of a patient. This patient was, in fact, a medical

student, with chronic myeloid leukaemia. The dramatic benefit from this treatment led to its use in a range of other blood malignancies. P-32 remains a useful treatment for myeloproliferative syndromes, especially in the elderly who tolerate chemotherapy poorly. In studying calcium metabolism using Sr-89, a Belgian by the name of Charles Pecher believed he had discovered a cure for metastatic prostate cancer following dramatic and complete pain relief in a patient suffering from advanced stages of this disease. Although this discovery was lost for a period of time due to a combination of the untimely death by suicide of Pecher and suppression of information about the American nuclear weapons program, it was “rediscovered” in the 1970s and was the first of a range of bone-seeking radiopharmaceuticals that came into widespread use in the 1980s and 1990s [2]. In studying thyroid function using I-130 in the 1930s, the development of hypothyroidism was recognised and leveraged for the treatment of thyrotoxicosis. Subsequently, Glenn Seaborg and John Livingood made I-131 and Sam Seidlin applied it to the treatment of metastatic thyroid cancer in the 1940s [3]. It has since become an integral part of the management of thyroid cancer. The ability to iodinate biologically relevant molecules was translated into other therapies including I-131 metaiodobenzylguanidine. I was privileged to be trained in therapeutic nuclear medicine at the University of Michigan by some of the pioneers of this therapy, James Sisson and Brahm Shapiro [4]. This treatment remains an important therapeutic option for the treatment of metastatic pheochromocytoma and paraganglioma and also in refractory neuroblastoma [5]. While these therapeutic techniques have continued to be used by nuclear medicine physicians, with the exception of I-131 therapy of thyroid cancer, they are often seen as the treatment of last resort after surgery, chemotherapy, targeted agents and radiotherapy have failed.

21.3 The Rise and Rise of Imaging

In evaluating the uptake and retention of I-131 in thyroid cancer metastases, Sam Seidlin used a Geiger-Muller counter since nuclear imaging hadn't been conceived. It wasn't until the advent of the rectilinear scanner, conceived by Benedict Cassen, that it became possible to image the internal distribution of radiopharmaceuticals. In the first of many seminal contributions to the field of nuclear medicine, David Kuhl combined photographic film to the rectilinear scanner to create the photoscanner [6]. He subsequently developed the principles of tomographic imaging while being a resident in the Radiology Department of the University of Pennsylvania [7]. Using an Am-245 source, he created the first transmission scan, a forerunner of X-ray computed tomography [8], and also performed emission tomography, the forerunner of single-photon emission computed tomography (SPECT) [9]. Gordon Brownell developed coincidence detection to acquire multiplanar images from positron-emitting radionuclides, and Michael Phelps and Ed Hoffman adopted this approach and combined it with the tomographic method developed by Kuhl to create positron emission tomography (PET). The first human

scanner was released in 1976 [10]. The real revolution in PET came with the development of the glucose analogue F-18 fluorodeoxyglucose (FDG) [11]. It was both fortunate and tragic that FDG was one of the first PET tracers to become available. Its excellent performance for evaluating diseases of the heart [12] and brain [13] and more recently cancer has stifled the clinical application of other PET tracers. Even its lack of specificity in whole-body imaging mode has found application for the imaging of infection and inflammation.

Throughout the world FDG PET/CT has become the dominant molecular imaging technique for evaluating cancer with demonstrated effectiveness in diagnosis, staging, therapeutic response assessment and restaging. Further, it provides information of about the biological aggressiveness of tumours. With the addition of anatomical landmarks from CT, some see FDG as the ideal “contrast agent” for cancer detection and has encouraged many to consider nuclear medicine as a diagnostic imaging technique that should be integrated into radiology. This view has been strengthened by the development of hybrid PET-MRI scanners, which have a particular strength in localisation of disease sites.

The wider availability of PET/CT scanners has, however, made positron-emitting radiopharmaceuticals that were developed and used in the era of rectilinear scanners but which fell out of favour with the introduction of the gamma camera, attractive again. F-18 sodium fluoride (NaF) was formerly a widely used agent for bone scanning but was replaced by Tc-99 m bisphosphonates in routine nuclear medicine practice as the gamma camera replaced rectilinear scanners. NaF PET/CT is, however, clearly superior to Tc-99 m MDP SPECT/CT in terms of spatial and contrast resolution, enhancing both sensitivity and specificity [14]. Gallium-68 is another example of an old radionuclide being seen in a new light and will be addressed later.

The major focus of much PET radiopharmaceutical development has, however, been on compounds labelled with fluorine-18. This is a radionuclide that is easily produced in small cyclotrons in abundant quantities after a relatively short period of target irradiation. Its physical half-life is attractive both for distribution and imaging. In my own department we chose to establish fluorinated PET tracers in addressing areas in which FDG has demonstrable weaknesses and the alternative SPECT agents are also suboptimal. As a result, the amino acid analogue, F-18 fluoro-ethyl-tyrosine (FET), which has low uptake in normal brain tissue but enhanced transport into brain tumours, has replaced both FDG PET and Tl-201 SPECT brain tumour imaging in our facility [15], as it has in many other centres [16]. Similarly, the proliferation tracer, F-18 fluorothymidine (FLT) provides a conceptually more robust evaluation of the status of bone marrow function than does a range of techniques previously used to assess this using a gamma camera. Whereas we previously utilised either radiolabelled white blood cells or Tc-99 m antimony colloid scanning, we now exclusively use FLT to assess bone marrow reserves [17] or to assess unexplained cytopenias. Preliminary data suggests a potential role of this agent for assessing leukaemias [18]. Similarly, agents such as F-18 fluoro-methyl-choline (FCH) have also found a clinical role in the evaluation of cancers that tend to have low uptake of the conventional oncological PET tracer,

Table 21.1 Fluorinated tracers used clinically at the Peter MacCallum Cancer Centre

Agent	Abbreviation	Process	Clinical use
¹⁸ F-fluoro-deoxyglucose	FDG	Glycolytic metabolism	Most cancers Neutropaenic sepsis
¹⁸ F-fluoro-thymidine	FLT	Cell proliferation	Marrow status Tumour proliferation
¹⁸ F-sodium fluoride	NaF	Bone formation	Prostate cancer, breast cancer, osteosarcoma etc.
¹⁸ F-fluoro-methyl-choline	FCH	Membrane synthesis	Prostate cancer, lobular breast cancer
¹⁸ F-fluoro-ethyl-tyrosine	FET	Amino acid transport	Brain tumours
¹⁸ F-fluoro-azomycin-aribinoside	FAZA	Hypoxia	Assessment for hypoxia cytotoxins

FDG [19]. Prostate cancer and lobular breast cancer are notable examples [20]. Table 21.1 provides a list of fluorinated agents routinely used in my department for oncological indications. We have a range of other F-18-labelled agents that are still being evaluated in clinical trials. These include an agent with high specificity for melanin, an attractive target for imaging malignant melanoma.

Despite the attraction of F-18, there remained many aspects of oncological imaging practice that were still best served by single-photon-emitting radionuclides. This situation has more recently been addressed by development of gallium-68-based tracers. The germanium-gallium-68 generator has reintroduced a radionuclide that was first described more than 50 years ago. Providing an alternative to the technetium-99 m generator, Ga-68 provides the option of centres without immediate access to a cyclotron, or even those with access to cyclotron products, to a potentially wide array of radiotracers that can replace existing nuclear medicine techniques.

The most established of these tracers are the somatostatin analogues, which have significantly impacted the management of patients with a range of neuroendocrine tumour (NET) [21]. Where available, these Ga-68 agents have largely replaced the conventional nuclear medicine imaging technique of In-111 DTPA-octreotide scintigraphy due to a combination of significantly enhanced diagnostic accuracy, greater patient convenience and more favourable radiation dosimetry. However, there is a range of other agents that could rapidly enter into routine nuclear medicine practice. These include agents for renal scanning [22] and ventilation-perfusion imaging [23]. Table 21.2 provides a list of Ga-68-labelled agents that are used clinically in my department.

There has also been a move to replace I-131, which has unfavourable imaging and radiation dose characteristics with I-123 for SPECT/CT diagnostic imaging. We clearly preferred this agent to I-131, but when comparing it to FDG, the technical differences between the scans often limited comparison of tracer avidity, particularly for small lesions. Accordingly, we have moved to using I-124, particularly in patients likely to come to I-131-based therapy. The treatment of metastatic thyroid cancer, pheochromocytoma/paraganglioma, neuroblastoma and

Table 21.2 Gallium-68 tracers used clinically at the Peter MacCallum Cancer Centre

Agent	Abbreviation	Process	Clinical use
⁶⁸ Ga-DOTA-octreotate	GaTate	SSTR	NET Phaeo/PGL
⁶⁸ Ga-DOTA-exendin-4	Ga-GLP-1	GLP-1 receptor	Insulinoma/MTC
⁶⁸ Ga-nano-aerosol	Galligas	Ventilation	VQ scanning
⁶⁸ Ga-macro-aggregated albumin	Ga-MAA	Lung perfusion	VQ scanning
⁶⁸ Ga-EDTA	Ga-EDTA	Renal filtration	Renal scanning
⁶⁸ Ga-HBED-PSMA	Ga-PSMA	PSMA cell surface expression	Prostate cancer Renal cancer
⁶⁸ Ga-nano-colloid	Ga-colloid	Phagocytosis	SLN imaging
⁶⁸ Ga-tropolone	Ga-RBC	Blood products	Blood pool imaging

SSTR somatostatin receptor, *NET* neuroendocrine tumour, *Phaeo/PGL* phaeochromocytoma/paraganglioma, *SNL* sentinel lymph node, *RBC* red blood cell

Table 21.3 Iodine-124 tracers used clinically at the Peter MacCallum Cancer Centre

Agent	Abbreviation	Process	Clinical use
¹²⁴ I-iodide	I-124	NaI symporter	Thyroid cancer
¹²⁴ I-meta-iodo-benzylguanidine	I-124 MIBG	Catecholamine transporter	Phaeo/PGL Neuroblastoma

Phaeo/PGL phaeochromocytoma/paraganglioma

lymphoma with iodinated products has opened the way for the “theranostic” application of I-124-labelled tracers. Table 21.3 provides a list of I-124 compounds used clinically in my department.

In addition to these tracers, we are involved in developing further agents for clinical PET scanning or validating agents that have been developed elsewhere. These include agents labelled with Cu-64 and Zr-89. These agents will play, we believe, an important role in further advancing the safety and efficacy of radionuclide therapy as well as putting it on a solid scientific footing. Table 21.4 provides a list of agents that are being evaluated prior to moving into routine clinical use.

This catalogue of tracers is not limited by opportunities for further relevant clinical applications but rather by the challenges posed by producing such a large array of tracers in an academic department, particularly in the context of increasingly stringent requirements for product to comply with good manufacturing practice (GMP). We have partly overcome these issues by partnering with a commercial supplier of PET tracers who have helped to transition tracers from the research domain into routine clinical practice by producing and distributing GMP-certified agents more widely. By achieving economies of scale not feasible in a hospital-based radiopharmacy, tracers like FLT, FET and NaF are now readily available to other PET facilities in our region. As experience with these tracers has grown, the role of PET has become ever more enthusiastically embraced by medical

Table 21.4 Other tracers being evaluated at the Peter MacCallum Cancer Centre

Agent	Abbreviation	Process	Clinical use
¹⁸ F-Fluoronicotinamide	MEL-50	Melanin	Melanoma
⁶⁴ Cu-SAT-octreotate	CuSARTATE	SSTR	NET
⁷⁹ Zr-trastuzumab	Zr-CEPTIN	HER-2 receptor	Breast cancer
¹²⁴ I-metomidate	I-124 rituxan	Cortisol synthesis	Adrenocortical cancer

SSTR somatostatin receptor, *NET* neuroendocrine tumour

and radiation oncologists as well as by surgeons. There are, in many countries, impediments to dissemination of these techniques as a result of health technology assessment regimes that require a significantly higher level of evidence than existed for older technologies prior to allowing their use and, particularly, reimbursing their cost. Notwithstanding these limitations, it seems inevitable that hybrid PET devices will become the preferred diagnostic imaging technique in cancer at least [24].

21.4 The Slow Rebirth of Radionuclide Therapy

Many hoped that small-molecule kinase inhibitors that target specific mutations in cancer cells would be the final solution in cancer therapy. The dramatic metabolic responses seen in gastrointestinal stromal tumours (GISTs) provided great excitement, as this was a disease previously without effective therapies. The use of BRAF inhibitors to combat the most common mutation in malignant melanoma was similarly ground-breaking and again accompanied by marked and early metabolic response in FDG PET [25]. However, it has become very clear that resistance to such agents develops almost universally, sometimes after only a brief response. This resistance arises due to genomic heterogeneity and evolution of tumours under the selective pressure of signal transduction blockade. If cells lack the specific therapeutic target or develop a means of bypassing its role in promoting tumour growth, the therapy ceases to work. Similarly, if delivery of the drug to the tumour is impaired, inadequate drug levels may allow cells to survive. While radionuclide therapy also relies on target expression, it is possible to measure the expression of any given target in individual lesions serially over time and on a whole-body scale. Thus, the task of selecting patients for radionuclide therapy and predicting which lesions will respond, and those that are unlikely to, is significantly easier than it is for targeted therapies where treatment selection is typically made on the basis of a tiny piece of biopsy material, which is assumed to be representative of all sites of disease. Furthermore, unlike drugs that require each cell to express the target, the particle range of many therapeutic isotopes means that a cell with high uptake can lethally irradiate nearby cancer cells that might themselves either lack the target or take up insufficient of the agent to have a direct toxic effect. The recognition of microscopic tissue heterogeneity within tumours provides a strong rational basis for

radionuclide therapy with crossfire effect overcoming spatial heterogeneity of target expression, at least at the microscopic scale.

While the old war horses, I-131 and Y-90, remain important therapeutic radionuclides, the renaissance of radionuclide therapy has been driven by the development of Lu-177. The physical characteristics of this isotope make it highly attractive for therapy. Although it has sufficient gamma emissions to allow reasonably high-quality post-therapy imaging, they are not so abundant to pose a major external radiation hazard allowing treatment to usually be performed on an outpatient basis. The decay rate delivers radiation over several weeks but the beta-particle range of only 1–2 mm means that relatively little radiation is delivered to normal cells close to tumour deposits. This is especially beneficial for treating patients with rather heavy infiltration of the liver or bone marrow. Recent studies have also indicated the potential of alpha-particle-emitting radionuclides such as Ra-223 [26], which deliver radiation over only a few cell diameters.

Lu-177 DOTA-octreotate (LuTate) has revolutionised our treatment of NET. Building on the pioneering work of the Erasmus Medical Center in Rotterdam, Holland, we added radiosensitising chemotherapy to the therapeutic regimen [27] and have achieved excellent progression-free and overall survival rates even in patients who would be considered to have a poor prognosis based on the presence of high FDG avidity [28]. The key to achieving such outcomes has, however, been ensuring that there are no lesions with FDG uptake that lack sufficient somatostatin receptor to deliver effective radiation [29]. Again, this reflects a cogent example of the theranostic paradigm wherein personalised selection of treatment can be based on “if you can see it, you can treat it”.

Another example of this approach has been the development of PSMA-binding ligands that are labelled with either I-131 [30] or Lu-177 [31]. Although preliminary, the results look impressive in patients with advanced castrate-resistant prostate cancer. As is often the case, the patients referred for such trials have often been heavily pretreated with several lines of therapy and have large burdens of disease. Our own “compassionate use” eligibility criteria similarly allowed treatment of patients who would almost certainly be ineligible for most industry-sponsored trials of novel chemotherapy or targeted agents.

Herein lies a major future issue for nuclear medicine. We see patients who are often at death’s door; we usually referred them only when another oncologist has effectively abandoned the patient’s care for lack of any other options and has little incentive to ever see the patient again. We see the wonderful benefit that some, indeed many, patients derive, but this is usually reported in case series that lack rigorous prospective design, defined eligibility criteria or standardised response and toxicity assessment. Accordingly, the medical community often view these trials as being flawed at best and anecdotal at worst.

If we are going to have radionuclide therapy assume the respectability it deserves as a cancer therapy, we need to adopt the trial methodology used by drug companies and stick to clearly defined protocols. There are certainly encouraging moves in this direction with both industry-funded and cooperative group trials being developed that integrate radionuclide therapy.

21.5 Long-Lived PET Isotopes with Therapeutic Pairs Provide the Vehicle for Improved Radionuclide Therapy Selection and Planning

One of the major impediments to establishing a scientific foundation for radionuclide therapy has been the inability to both predict and verify the radiation dose delivered to both tumour and normal tissues. Although planar imaging has been able to provide estimates of radiation to normal organs, the development of three-dimensional and quantitative capability of hybrid scanners have made it possible to use PET/CT to perform predictive dosimetry while quantitative SPECT/CT is being refined to allow dose verification.

My group has established methods for quantitative Lu-177 SPECT/CT [32]. This has taught us that while uptake of GaTate on pretreatment PET/CT provides a reasonable estimate of what radiation will be delivered to tumour deposits, it is clear that clearance kinetics of normal organs, particularly the kidneys, varies considerably between patients and cannot be adequately modelled using short-lived tracers. This is where longer-lived PET radionuclides will play an important role. For predictive dosimetry of I-131 agents, I-124 provides the ideal combination of a reasonably comparable physical half-life and excellent imaging characteristics. Cu-64 provides an interesting opportunity for predictive dosimetry of its therapeutic pair Cu-67 but could also be used as a PET surrogate for Lu-177 [33]. Zr-89 and Y-90 provide another interesting combination with respect to radioimmunotherapies.

In the future, the theranostic paradigm will hopefully change from a rather empiric approach of “see it, guess an administered activity and treat it in hope” to one that could be characterised as “see it, measure it, predict and verify therapeutic radiation delivery within tolerance of normal tissues”. As is often the case, the past can teach us useful lessons.

Open Access This chapter is distributed under the terms of the Creative Commons Attribution-Noncommercial 2.5 License (<http://creativecommons.org/licenses/by-nc/2.5/>) which permits any noncommercial use, distribution, and reproduction in any medium, provided the original author(s) and source are credited.

The images or other third party material in this chapter are included in the work's Creative Commons license, unless indicated otherwise in the credit line; if such material is not included in the work's Creative Commons license and the respective action is not permitted by statutory regulation, users will need to obtain permission from the license holder to duplicate, adapt or reproduce the material.

References

1. Seaborg GT, Lawrence EO. Physicist, engineer, statesman of science. *Science*. 1958;128(3332):1123–4. doi:10.1126/science.128.3332.1123.
2. Robinson RG, Blake GM, Preston DF, McEwan AJ, Spicer JA, Martin NL, et al. Strontium-89: treatment results and kinetics in patients with painful metastatic prostate and breast cancer in bone. *Radiographics*. 1989;9(2):271–81. doi:10.1148/radiographics.9.2.2467331.

3. Seidlin SM, Marinelli LD, Oshry E. Radioactive iodine therapy; effect on functioning metastases of adenocarcinoma of the thyroid. *J Am Med Assoc.* 1946;132(14):838–47.
4. Shapiro B, Sisson JC, Eyre P, Copp JE, Dmuchowski C, Beierwaltes WH. 131I-MIBG—a new agent in diagnosis and treatment of pheochromocytoma. *Cardiology.* 1985;72 Suppl 1:137–42.
5. Shulkin BL, Shapiro B. Current concepts on the diagnostic use of MIBG in children. *J Nucl Med.* 1998;39(4):679–88.
6. Kuhl DE, Chamberlain RH, Hale J, Gorson RO. A high-contrast photographic recorder for scintillation counter scanning. *Radiology.* 1956;66(5):730–9.
7. Kuhl DE, Edwards RQ. Cylindrical and section radioisotope scanning of the liver and brain. *Radiology.* 1964;83:926–36.
8. Kuhl DE, Hale J, Eaton WL. Transmission scanning: a useful adjunct to conventional emission scanning for accurately keying isotope deposition to radiographic anatomy. *Radiology.* 1966;87(2):278–84.
9. Kuhl DE, Edwards RQ, Ricci AR, Jacob RJ, Mich TJ, Alavi A. The Mark IV system for radionuclide computed tomography of the brain. *Radiology.* 1976;121(2):405–13.
10. Phelps ME, Hoffman EJ, Huang SC, Kuhl DE. Positron tomography: “in vivo” autoradiographic approach to measurement of cerebral hemodynamics and metabolism. *Acta Neurol Scand Suppl.* 1977;64:446–7.
11. Reivich M, Kuhl D, Wolf A, Greenberg J, Phelps M, Ido T, et al. Measurement of local cerebral glucose metabolism in man with 18F-2-fluoro-2-deoxy-d-glucose. *Acta Neurol Scand Suppl.* 1977;64:190–1.
12. Phelps ME, Hoffman EJ, Selin C, Huang SC, Robinson G, MacDonald N, et al. Investigation of [18F]2-fluoro-2-deoxyglucose for the measure of myocardial glucose metabolism. *J Nucl Med.* 1978;19(12):1311–9.
13. Reivich M, Kuhl D, Wolf A, Greenberg J, Phelps M, Ido T, et al. The [18F]fluorodeoxyglucose method for the measurement of local cerebral glucose utilization in man. *Circ Res.* 1979;44(1):127–37.
14. Schirrmester H, Glatting G, Hetzel J, Nussle K, Arslandemir C, Buck AK, et al. Prospective evaluation of the clinical value of planar bone scans, SPECT, and (18)F-labeled NaF PET in newly diagnosed lung cancer. *J Nucl Med.* 2001;42(12):1800–4.
15. Lau EW, Drummond KJ, Ware RE, Drummond E, Hogg A, Ryan G, et al. Comparative PET study using F-18 FET and F-18 FDG for the evaluation of patients with suspected brain tumour. *J Clin Neurosci.* 2010;17(1):43–9. doi:[10.1016/j.jocn.2009.05.009](https://doi.org/10.1016/j.jocn.2009.05.009).
16. Popperl G, Gotz C, Rachinger W, Gildehaus FJ, Tonn JC, Tatsch K. Value of O-(2-[18F]fluoroethyl)- L-tyrosine PET for the diagnosis of recurrent glioma. *Eur J Nucl Med Mol Imaging.* 2004;31(11):1464–70.
17. Campbell BA, Callahan J, Bressel M, Simoens N, Everitt S, Hofman MS, et al. Distribution atlas of proliferating bone marrow in non-small cell lung cancer patients measured by FLT-PET/CT imaging, with potential applicability in radiation therapy planning. *Int J Radiat Oncol Biol Phys.* 2015;92(5):1035–43. doi:[10.1016/j.ijrobp.2015.04.027](https://doi.org/10.1016/j.ijrobp.2015.04.027).
18. Buck AK, Bommer M, Juweid ME, Glatting G, Stilgenbauer S, Mottaghy FM, et al. First demonstration of leukemia imaging with the proliferation marker 18F-fluorodeoxythymidine. *J Nucl Med.* 2008;49(11):1756–62. doi:[10.2967/jnumed.108.055335](https://doi.org/10.2967/jnumed.108.055335).
19. Price DT, Coleman RE, Liao RP, Robertson CN, Polascik TJ, DeGrado TR. Comparison of [18 F]fluorocholine and [18 F]fluorodeoxyglucose for positron emission tomography of androgen dependent and androgen independent prostate cancer. *J Urol.* 2002;168(1):273–80.
20. Beauregard JM, Williams SG, DeGrado TR, Roselt P, Hicks RJ. Pilot comparison of F-fluorocholine and F-fluorodeoxyglucose PET/CT with conventional imaging in prostate cancer. *J Med Imaging Radiat Oncol.* 2010;54(4):325–32. doi:[10.1111/j.1754-9485.2010.02178.x](https://doi.org/10.1111/j.1754-9485.2010.02178.x).
21. Hofman MS, Kong G, Neels OC, Eu P, Hong E, Hicks RJ. High management impact of Ga-68 DOTATATE (GaTate) PET/CT for imaging neuroendocrine and other somatostatin expressing tumours. *J Med Imaging Radiat Oncol.* 2012;56(1):40–7. doi:[10.1111/j.1754-9485.2011.02327.x](https://doi.org/10.1111/j.1754-9485.2011.02327.x).

22. Hofman M, Binns D, Johnston V, Siva S, Thompson M, Eu P, et al. ⁶⁸Ga-EDTA PET/CT imaging and plasma clearance for glomerular filtration rate quantification: comparison to conventional ⁵¹Cr-EDTA. *J Nucl Med.* 2015;56(3):405–9. doi:[10.2967/jnumed.114.147843](https://doi.org/10.2967/jnumed.114.147843).
23. Callahan J, Hofman MS, Siva S, Kron T, Schneider ME, Binns D, et al. High-resolution imaging of pulmonary ventilation and perfusion with ⁶⁸Ga-VQ respiratory gated (4-D) PET/CT. *Eur J Nucl Med Mol Imaging.* 2014;41(2):343–9. doi:[10.1007/s00259-013-2607-4](https://doi.org/10.1007/s00259-013-2607-4).
24. Hicks RJ, Hofman MS. Is there still a role for SPECT-CT in oncology in the PET-CT era? *Nat Rev Clin Oncol.* 2012;9(12):712–20. doi:[10.1038/nrclinonc.2012.188](https://doi.org/10.1038/nrclinonc.2012.188).
25. McArthur GA, Puzanov I, Amaravadi R, Ribas A, Chapman P, Kim KB, et al. Marked, homogeneous, and early [¹⁸F]fluorodeoxyglucose-positron emission tomography responses to vemurafenib in BRAF-mutant advanced melanoma. *J Clin Oncol.* 2012;30(14):1628–34. doi:[10.1200/JCO.2011.39.1938](https://doi.org/10.1200/JCO.2011.39.1938).
26. Parker C, Nilsson S, Heinrich D, Helle SI, O’Sullivan JM, Fosså SD, et al. Alpha emitter radium-223 and survival in metastatic prostate cancer. *N Engl J Med.* 2013;369(3):213–23. doi:[10.1056/NEJMoa1213755](https://doi.org/10.1056/NEJMoa1213755).
27. Kong G, Thompson M, Collins M, Herschtal A, Hofman MS, Johnston V, et al. Assessment of predictors of response and long-term survival of patients with neuroendocrine tumour treated with peptide receptor chemoradionuclide therapy (PRCRT). *Eur J Nucl Med Mol Imaging.* 2014;41(10):1831–44. doi:[10.1007/s00259-014-2788-5](https://doi.org/10.1007/s00259-014-2788-5).
28. Kashyap R, Hofman MS, Michael M, Kong G, Akhurst T, Eu P, et al. Favourable outcomes of (¹⁷⁷)Lu-octreotate peptide receptor chemoradionuclide therapy in patients with FDG-avid neuroendocrine tumours. *Eur J Nucl Med Mol Imaging.* 2015;42(2):176–85. doi:[10.1007/s00259-014-2906-4](https://doi.org/10.1007/s00259-014-2906-4).
29. Hofman MS, Hicks RJ. Changing paradigms with molecular imaging of neuroendocrine tumors. *Dis Med.* 2012;14(74):71–81.
30. Zechmann CM, Afshar-Oromieh A, Armor T, Stubbs JB, Mier W, Hadaschik B, et al. Radiation dosimetry and first therapy results with a (¹²⁴)I/ (¹³¹)I-labeled small molecule (MIP-1095) targeting PSMA for prostate cancer therapy. *Eur J Nucl Med Mol Imaging.* 2014;41(7):1280–92. doi:[10.1007/s00259-014-2713-y](https://doi.org/10.1007/s00259-014-2713-y).
31. Kratochwil C, Giesel FL, Eder M, Afshar-Oromieh A, Benešová M, Mier W, et al. [¹⁷⁷)Lu] Lutetium-labelled PSMA ligand-induced remission in a patient with metastatic prostate cancer. *Eur J Nucl Med Mol Imaging.* 2015;46(2):987–8.
32. Beauregard JM, Hofman MS, Pereira JM, Eu P, Hicks RJ. Quantitative (¹⁷⁷)Lu SPECT (QSPECT) imaging using a commercially available SPECT/CT system. *Cancer Imaging.* 2011;11:56–66. doi:[10.1102/1470-7330.2011.0012](https://doi.org/10.1102/1470-7330.2011.0012).
33. Paterson BM, Roselt P, Denoyer D, Cullinane C, Binns D, Noonan W, et al. PET imaging of tumours with a ⁶⁴Cu labeled macrobicyclic cage amine ligand tethered to Tyr³-octreotate. *Dalton Trans.* 2014;43(3):1386–96. doi:[10.1039/c3dt52647j](https://doi.org/10.1039/c3dt52647j).

Chapter 22

Interactive Communication Between PET Specialists and Oncologists

Huiting Che, Ying Zhang, Ying Dong, Wensheng Pan, Ling Chen, Hong Zhang, and Mei Tian

Abstract With an increasing number of positron emission tomography (PET) facilities while a growing shortage of PET specialists in mainland China, interactive communication between PET specialists and oncologists plays a crucial role in individualized management of cancer patients and survivors. It is essential that PET specialists should be well informed by oncologists of their patients' history, current problem, treatments, and particularly, the follow-up information. Vice versa, oncologists should be advised by PET specialists on their thorough interrogation, detailed observations, as well as potential false-positive or false-negative findings – some of which might be ignored in their reports. Improving communication and coordination between PET specialists and oncologists has been linked not only to greater understanding and cooperation but also better patient management. In addition, this interactive communication is an essential element of good collaboration for multi-center clinical trials, for instance, how to make PET as an imaging biomarker to evaluate efficacy more rapidly and to increase the probability of success in a clinical trial and how to move non-FDG radiopharmaceutical forward, etc. Here, our review focuses on the conceptual framework, key features, current problems, and future perspectives on this topic.

H. Che • Y. Zhang • L. Chen • H. Zhang • M. Tian (✉)

Department of Nuclear Medicine, The Second Affiliated Hospital of Zhejiang University School of Medicine, 88 Jiefang Road, Hangzhou, Zhejiang 310009, China

Zhejiang University Medical PET Center, 88 Jiefang Road, Hangzhou, Zhejiang 310009, China

Institute of Nuclear Medicine and Molecular Imaging of Zhejiang University, Hangzhou, China

Key Laboratory of Medical Molecular Imaging of Zhejiang Province, Hangzhou, China
e-mail: meitian@zju.edu.cn

Y. Dong

Department of Oncology, The Second Affiliated Hospital of Zhejiang University School of Medicine, Hangzhou, China

W. Pan

Department of Digestive Disease, The Second Affiliated Hospital of Zhejiang University School of Medicine, Hangzhou, China

Keywords Positron emission tomography (PET) • Interdisciplinary communication • Patient care management

22.1 Introduction

With an increasing number of positron emission tomography (PET) facilities while a growing shortage of PET specialists in China, interactive communication between PET specialists and oncologists plays a crucial role in individualized management of cancer patients and survivors [1]. In most of clinical settings, cancer patients receive direct or indirect care from a multidisciplinary medical team, including PET specialists and oncologists. The interactive communication regarding patient care is extremely important for diagnostic consistency and therapeutic efficiency [2]. Usually, oncologists select their therapeutic strategy largely on patient history, laboratory tests, and imaging studies including X-ray, ultrasound (US), computed tomography (CT), magnetic resonance imaging (MRI), single photon emission computed tomography (SPECT), or hybrid imaging modalities (i.e., SPECT/CT, PET/CT, or PET/MRI) [3]. PET specialists commonly use PET/CT with ^{18}F -FDG or other radiolabeled imaging agents to evaluate the accumulation or binding activity of a particular biological target or evaluate the functional or metabolic changes after a certain kind of therapy. Among all the current commercially available PET imaging agents, ^{18}F -FDG, the most commonly and widely used in the clinic, has the highest sensitivity, specificity, or accuracy in detecting many glucose-avid cancers compared to the other conventional anatomical imaging modalities. By visualized or semiquantitative analysis of the biochemical or biophysical information on whole-body PET images, PET specialists are being able to not only provide an accurate cancer stage (pinpoint the primary and/or metastatic lesions throughout the body) but also help to select particular targeted patients for the targeted therapy [4–7]. In addition, PET is helpful to assess a specific therapeutic efficacy and detect metastasis or recurrence much earlier than the other imaging modalities in many common cancers [8–11]. Obviously, in every process of patients' management, PET specialists could provide assistance to oncologists. Therefore, a strong cooperative relationship between them can offer efficient care to the cancer patients.

22.2 Oncologists

Defined in the American Society of Clinical Oncology (ASCO), an oncologist is a physician who is specialized in treating people with cancer [12]. There are three major types of oncologists: medical, surgical, and radiation. A medical oncologist is specialized in treating cancer with chemo-, immuno-, hormonal, or targeted therapy, while a surgical oncologist is specialized in the removal of the tumor and surrounding related tissues. And a radiation oncologist is specialized in radiation

therapy. Usually, these different types of oncologists need to work together in a relative late stage of cancer patient management.

22.3 PET Specialists and ^{18}F -FDG PET/CT

A PET specialist is a physician who is specialized in selecting the optimal imaging agent and acquisition protocol, interpreting PET or PET/CT images on the basis of physiological and biochemical information of the whole body and localized organs or tissues. In China, with an increasing number of PET facilities and lacking of PET specialists, most of the new PET specialists have been working as radiologists. From their point of view, PET may equal to the contrast CT or enhanced MRI. Nevertheless, they admit that PET is an important imaging approach in cancer patient management.

PET/CT technology is a novel combined method by which functional molecular information (PET) and anatomical information (CT) can be achieved simultaneously [4]. There are many radiotracers that can be used for PET/CT imaging, including ^{18}F -FDG, ^{18}F - or ^{11}C -acetate, ^{18}F - or ^{11}C -choline, etc. [13]. ^{18}F -FDG is the most widely used radiolabeled agent (or tracer) which is actively taken up and accumulated in cancer cells [4]. Since ^{18}F -FDG PET/CT can detect cancer cells at cellular and molecular levels, it is regarded as the most sensitive and specified method among current imaging modalities [14–16].

22.4 Important Roles of Oncologists and PET Specialists

Cancer is a group of disease, involving abnormal cell growth with the potential to invade or spread to other parts of the body [17]. In clinical practice, when a patient comes for unknown reasons like fever, weight loss, fatigue or elevated tumor markers, abnormal findings on US or X-ray, or in physical examinations, an experienced physician will consider “cancer” as one of her/his assumptions. If the patient has risk factors to cancer, oncologists will order specific laboratory tests and imaging examinations (including PET/CT, if available) for the patient. With patient’s medical history and PET/CT images, PET specialists can provide a valuable diagnosis for oncologists. If the patient is confirmed as having cancer, the oncologist will choose an appropriate treatment for him. After the treatment, PET specialists can evaluate its efficacy with PET or PET/CT. If the treatment is effective, the patient will be followed up for a certain period of time, otherwise, the oncologists will help the patient to choose another plan. Usually, during the post-therapeutic follow-up, PET specialists can use PET or PET/CT to detect the functional or metabolic change or recurrence much earlier than other imaging modalities (Fig. 22.1).

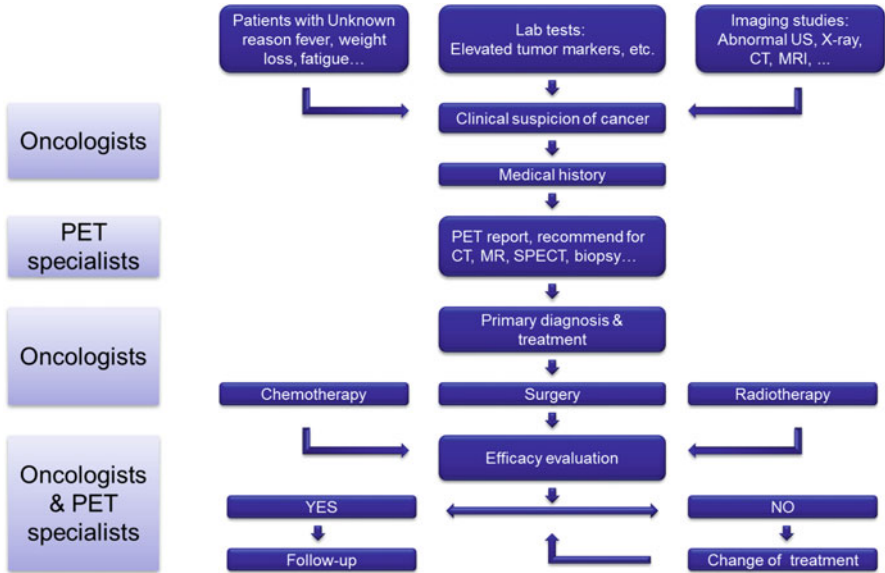


Fig. 22.1 Important roles of oncologists and PET specialists in cancer patient management

22.5 Communication Process

Communication is the process of passing information from a source to a receiver, which is classified into two models: linear and interactive. For the linear model, information is transmitted from sender to receiver via a channel without the sender receiving any feedback, i.e., PET specialist → report → oncologist → patient referring → PET specialist. While for the interactive model, it allows the sender to know that the message was received, i.e.: PET specialist ↔ oncologist. Interactive communication between PET specialists and oncologists allows these two groups to determine if the message was received and how accurately it was received.

Interactive communication is also considered as teamwork, which has the following characteristics:

1. Mutual respect and trust between team members
2. An equal voice for all members – different opinions valued
3. Resolution of conflict between team members
4. Encouragement of constructive discussion or debate
5. Ability to request and provide clarification if anything is unclear

22.6 What PET Specialists Can Do for Oncologists

PET specialists can effectively provide assistance for oncologists, such as (1) offering valuable diagnosis with important functional or metabolic information; (2) providing noninvasive overview of cancer stage; (3) monitoring therapeutic response, especially for the early stage of functional or metabolic changes after treatment; (4) follow-up and metastasis or recurrence detection; and (5) collaborating for clinical trials or other research projects.

22.6.1 Offering Valuable Diagnostic Information

A correct diagnosis is the key to suitable treatment. However, when a patient presenting nonspecific signs or symptoms (i.e., fever, tiredness, or weight loss) and when traditional imaging (i.e., X-ray, US, CT, or MRI) results are negative or controversial, PET or PET/CT could be used for an alternative diagnostic approach, and therefore, PET specialists can offer functional or metabolic diagnostic information to oncologists [18, 19].

Here is a case with unknown reason fever (Case 1):

A 71-year-old female patient who was admitted to the Department of Internal Medicine for fever with unknown reason. The fever lasted for 18 days and was treated with cefmetazole. The peak temperature reached 38.4 °C. In addition, she had a history of right hip pain 2 days prior to her fever. On her physical examination, she presented right hip tenderness without erythema, edema, or plump. On the laboratory results, tumor markers and other tests were in normal limits. She had performed Doppler ultrasound in the abdomen, lower limb arteries and deep veins, and cardiovascular and urinary systems with no remarkable findings. CT and enhanced MR in pelvic indicated a right iliac fossa abscess. In order to explore the cause to fever, she had a whole-body ¹⁸F-FDG PET/CT scan. Surprisingly on PET/CT images, her ascending colon showed a hypermetabolic mass which was suspected for colon cancer (A). Therefore, she had colonoscopy that found a polypoid lesion (Is + IIc lesion) of 15-mm diameter in the ascending colon, with hyperemia and pedunculus (Fig. 22.2B). The patient and her family requested for an operation. After the operation, routine hematoxylin and eosin (HE) staining confirmed “moderately differentiated adenocarcinoma” with submucosal invasion (Fig. 22.2C).

For the suspected cancer patients with positive lab tests or imaging findings, the golden standard of diagnosis is pathological confirmation, which needs surgical resection or biopsy. Since these invasive operations might increase the risk of cancer spreading, and false-negative results may occur especially in a heterogeneous large lesion, noninvasive and sensitive imaging techniques are extremely

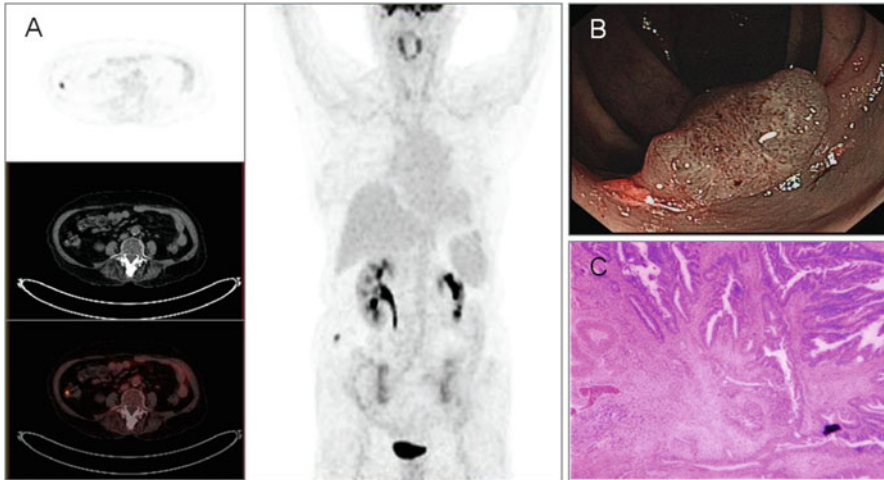


Fig. 22.2 (a) ^{18}F -FDG PET/CT images showed an area of intensive abnormal ^{18}F -FDG uptake in the ascending colon (*arrows*) with $\text{SUV}_{\text{max}} = 6.00(1\text{ h}), 9.52(2\text{ h})$. There was no increased ^{18}F -FDG uptake in the right lower limb. (b) Colonoscopy image. (c) Hematoxylin and eosin (HE) staining

needed. Since ^{18}F -FDG is actively accumulated in glucose-avid cancer cells, it could distinguish these cancer cells from the other noncancerous cells [4, 20]. Therefore, by using PET/CT imaging, PET specialists could offer valuable diagnostic information for oncologists.

22.6.2 Noninvasive Overview of Cancer Staging

Oncologists make treatment plan depending on various factors, for instance, a certain type of cancer, stage, gender, age, etc. Among these factors, cancer stage is the most crucial but most difficult to determine. Incorrect cancer stage will lead to poor prognosis of the patient. Underestimating the stage of the disease may lead to “positive resection margins” or unnecessary laparotomy, while overestimation of the stage may yield to ineffective treatment [21]. Although PET imaging studies are costly, it provides oncologists with important noninvasive overview of staging for making optimal choice of cancer patients.

For example, to determine the stage of non-small-cell lung cancer (NSCLC), multiple laboratory tests and imaging exams are required. Among all these examinations, high-resolution CT is currently the most frequently used in clinic. However, even if this imaging approach could provide accurate assessment of local tumor depth invasion (T), it lacks sensitivity and specificity in the assessment of

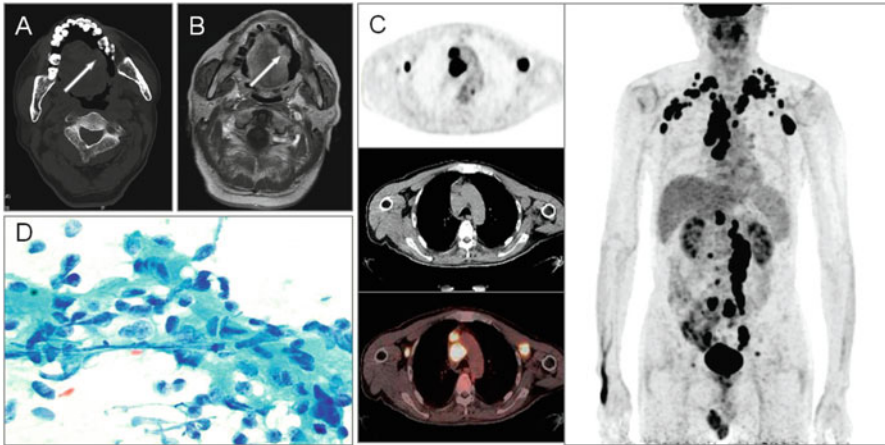


Fig. 22.3 (a) CT imaging detected a mass located in the left edge of the tongue (*arrow*). (b) MR imaging revealed a mass with long T1 and long T2 signals on the left edge of tongue, a size of 20-mm*10-mm, ill-defined margins (*arrow*). (c) ^{18}F -FDG PET/CT imaging showed intensive FDG uptake in the left tongue (SUVmax = 13.83), clavicle and axillary lymph nodes (SUVmax = 16.26), mediastinum (SUVmax = 17.35), ventral prostate (SUVmax = 14.40 at 1 h and SUVmax = 20.46 at 2 h post ^{18}F -FDG injection), in retroperitoneum, bottom of mesentery, and left inguinal region's lymph nodes (SUVmax = 21.47). (d) Fine needle aspiration confirmed for squamous cell carcinoma

regional lymph node invasion (N) and distant metastasis (M). Although PET only is not so effective in assessing T, it has great superiority in assessing N and M. Recently, hybrid PET/CT has become one of the optimal imaging technologies for lung cancer staging, and significantly improved the detectability of local and distant metastases in patients with NSCLC, and reduced both the total number of thoracotomies and the number of futile thoracotomies [5, 22–24].

Here is a case of a tongue cancer patient with distant metastases (Case 2):

A 68-year-old male patient who was admitted to the Department of Oral and Maxillofacial Surgery. The patient presented left tongue ulcer for two months; incisional biopsy confirmed the diagnosis of squamous cell carcinoma in left ventral tongue at 1 week before PET/CT scan. On physical examination, his vital signs were normal, and he presented a size of 20-mm*18-mm, firm, ill-defined, and cauliflower-like neoplasm located in the left ventral tongue with obvious tenderness, but no palpable enlarged lymph nodes were found. On laboratory workup, PSA was 196.89 ng/ml and other tests were within the normal limits. After performing the head and neck CT and MR examinations (Fig. 22.3a and b), he was intended to have a surgical operation. However, the presurgical PET/CT indicated distant metastases (Fig. 22.3c). Therefore, he was performed a fine needle aspiration in the enlarged left inguinal lymph node and confirmed the diagnosis of metastasis from the left tongue (Case 2, Fig. 22.3d). Accordingly, he was treated with chemotherapy and radiotherapy.

Through the preoperative communication between the PET specialist and the oncologist, this patient avoided unnecessary surgery and administrated optimal care plan. Namely, with the noninvasive overview on ^{18}F -FDG PET/CT images, PET specialists are able to provide functional or metabolic information on T, but also more important information on N and M stages by the whole-body or total body images [25, 26].

22.6.3 Monitoring Efficacy of Treatments

The most common evaluation of a certain therapy to cancer is based on the initial diagnosis of TNM stage, which may reveal the current status and might predict the therapeutic outcome [27]. However, the morphologic and metabolic responses of cancer cells to a specific treatment are incongruent. For example, cetuximab and other targeted therapies inhibit cancer cell growth by inhibiting the proliferation, angiogenesis, and metastatic spread and by promoting apoptosis [28–30], which should be cytostatic rather than cytotoxic [27]. However, in many cases, especially in the early-phase post-therapy, the change of cellular or biochemical function may be significant, but a measurable reduction in tumor size may not occur. Therefore, tumor size can remain relatively unchanged while tumor metabolism can be markedly reduced immediately [31].

As a result, PET specialists play an important role in offering oncologists the real-time efficacy of a specific therapy and help oncologists to make adjustment to the current therapy or change to another option.

22.6.4 Detecting Metastasis or Recurrence in Follow-Up

The chance of survival depends on the type of cancer and extent of disease at the start of treatment. However, even with the rapid development of surgical, chemo-, radio-, hormonal, and gene therapy and targeted therapies, cancers cannot be completely cured in most cases [32]. Therefore, early detection of metastasis or recurrence is clinically important and helpful for improvement of the prognosis or survival of cancer patients [33].

Here is a case of non-Hodgkin's lymphoma with recurrence detected in the follow-up PET imaging (Case 3):

A 65-year-old Chinese female was admitted to the Department of Hematology for the right back pain which lasted for 2 weeks. She was diagnosed with non-Hodgkin's lymphoma 11 years ago and had an operation followed by six cycles of postoperative chemotherapy. Recurrence was detected 6 years ago and four cycles of chemotherapy was performed. One year prior to this admission, she had severe right back pain. ^{18}F -FDG PET/CT images found enlarged lymph

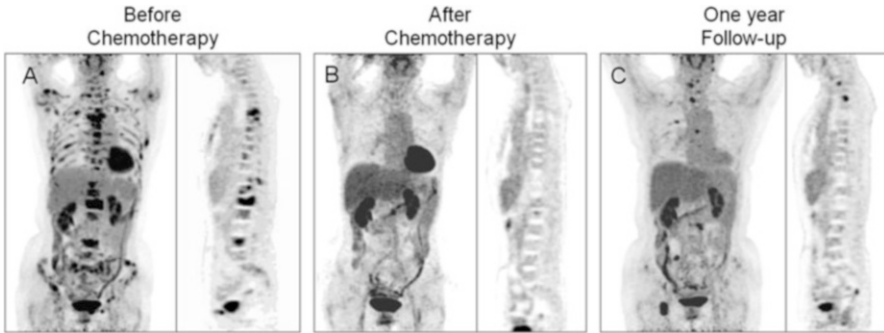


Fig. 22.4 (a) PET/CT showed increased FDG uptake in multiple bones, including sternum, vertebrae, ribs, pelvis, etc. with maximum SUV of 6.65 in the left clavicle, 11.70 in the L1 vertebra, 5.18 in the ribs, and 5.40 in the right ilium. (b) PET/CT images showed normal FDG uptake in the whole body. (c) PET/CT images presented intensive FDG uptake in bowels with SUVmax of 5.69–10.22 in bones

nodes in the neck and multiple bones (Fig. 22.4a). After that, vertebral body biopsy confirmed diffuse large B-cell lymphoma and indicated recurrent with transformation. Therefore, the patient was performed eight cycles of chemotherapy. Immediately after the completion of chemotherapy, PET/CT showed negative FDG uptake in all lymph nodes (Fig. 22.4b). For this time, the patient felt backache again, PET/CT revealed intensive FDG uptake in bones, bowels, and cervical lymph nodes, which indicated the recurrence (Fig. 22.4c).

At present, multiple studies found that increased tumor marker level do not indicate localization of cancer. Although increasing of tumor marker levels may be the earliest indication of recurrent cancer, false-positive results may be found in some benign and physiologic conditions as well. Thus, follow-up PET/CT scans have an impact on patient management since it can provide the extended whole-body functional overview of recurrence or metastasis [11, 34, 35].

22.6.5 Research Collaborations

PET, including small-animal (or micro) PET and clinical PET, has become a requisite of cancer research in this century. The most significant advantage of PET method is that radiolabeled imaging agent (or radiotracer) could penetrate into the cell and thus make it possible to reveal the *in vivo* biodistribution and biochemical process of living cells [4]. Furthermore, not only limited to FDG, a glucose analogue, there are many other radiotracers, for instance, ^{11}C -choline used in prostate carcinoma [36], ^{11}C -acetate used in hepatocellular carcinoma [37],

^{13}N -ammonia used in pancreatic necrosis [38], etc. Hence, with the assistance of different PET imaging tracers, PET specialists could help oncologists to visualize different targets in the living body and test the efficacy of novel treatment [39, 40].

22.7 What Oncologists Can Do for PET Specialists?

Oncologists can also provide assistance to PET specialists, such as (1) referring appropriate patients, (2) provide patient education and (3) provide more detailed patient medical history, and (4) scientific research collaboration.

22.7.1 Referring Appropriate Patients

PET is a highly sensitive imaging method for the detection of early stage of cancer, occult recurrence, and metastasis since cancer-related metabolic abnormalities usually precede structural changes and are readily detected by PET [33]. However, if without clear clinical indication, excessive PET scanning is likely to identify harmless findings that lead to more tests, biopsy, or unnecessary surgery. Therefore, referring appropriate cancer or suspicious patients for PET imaging is the key to get better prognosis for patients.

22.7.2 Providing Detailed Medical History

FDG is not a cancer-specific agent, and false-positive findings in benign diseases may occur [41–43]. Infectious diseases (mycobacterial, fungal, bacterial infection), sarcoidosis, radiation pneumonitis, and postoperative surgical conditions have shown intense uptake, while tumors with low glycolytic activity such as adenomas, bronchoalveolar carcinomas, carcinoid tumors, low-grade lymphomas, and small-sized tumors have revealed false-negative findings on PET images.

Here is a false-positive case with tuberculosis (Case 4):

A 22-year-old Chinese male was admitted to the thoracic surgical department for right chest pain. It is a moderate and tolerable pain presented after taking a deep breath which lasted for about 1 year. He had no smoking and drinking history. On physical examination, his vital signs were normal, and he presented rough breath sounds without any other symptoms. On laboratory tests, his T-SPOT test was positive, and other tests were in normal limits, including tumor markers. He had performed X-ray and high-resolution CT in the chest. High-resolution CT indicated a 13-mm*6-mm nodule in the lateral segment of the right middle lung (Fig. 22.5b). In order to determine whether the nodule was of malignant

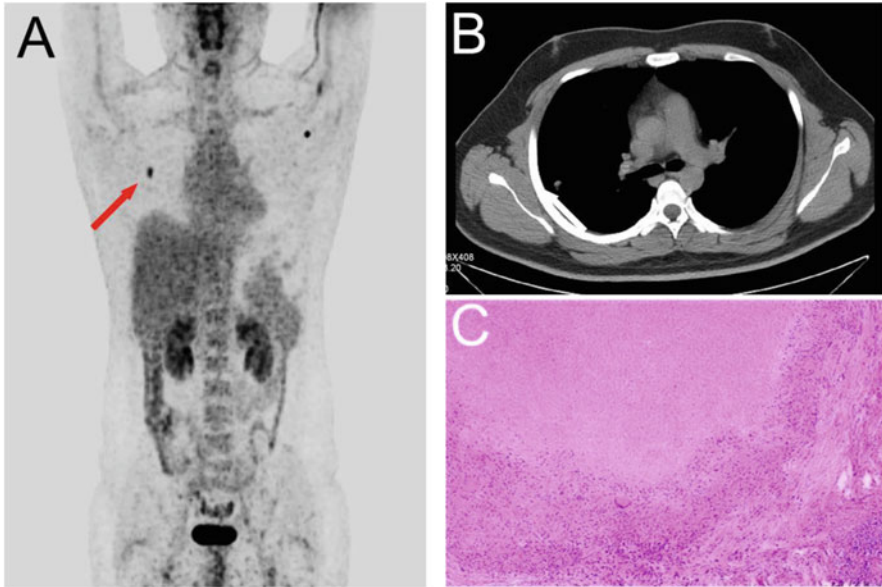


Fig. 22.5 (a) ^{18}F -FDG PET/CT images demonstrated a 12.9-mm*7.7-mm mass of intensive FDG uptake in the right middle lung (*red arrow*) with $\text{SUV}_{\text{max}} = 5.33$. (b) Diagnostic CT image showed a 13-mm*6-mm nodule in the lateral segment of the right middle lung. (c) Routine pathology of the mass revealed “chronic granulomatous inflammation”

etiology, the patient was referred for ^{18}F -FDG PET/CT imaging. On PET/CT images, a 12.9-mm*7.7-mm mass with intensive ^{18}F -FDG uptake was found in the lateral segment of the right middle lung (Fig. 22.5a). Based on the medical history (young man, nonsmoking, and moderate symptom), the PET specialist highly suspected for nonneoplastic diseases, such as tuberculosis or other inflammation despite the increased SUV value. However, the patient preferred to perform surgical resection. The pathological diagnosis verified it was inflammatory pseudotumor, tuberculosis (Fig. 22.5c).

22.7.3 Research Collaboration

PET is a functional molecular imaging technique which is based on radionuclide imaging of regional biochemistry *in vivo*. Biochemistry is considered the basis of diagnosis and of the planning and monitoring of treatment since the treatment of many diseases involves biochemical reactions. A number of radiolabeled PET tracers have been designed and developed to imaging the functional and biochemical process of tissues or cells which can be applied for experimental or clinical research, and can be initiated by either PET specialists or oncologists. The hybrid PET/CT not only can provide highly spatial resolution but also can reflect abnormal lesions, glucose, amino acid, nucleic acid, and gene. It is the only current imaging

method available from a physiological perspective and the molecular level for quantitative evaluation of biochemical changes. Oncologists pay more attention to the efficacy of different therapies, while PET specialists focus more on the applications of various radiotracers. Through collaborative research and interactive communication, PET specialists and oncologists may explore more on underlying mechanism of cancers.

22.8 Future Perspectives

Awareness of the impact of interactive communication between PET specialists and oncologists, particularly on patient referring, monitoring, and follow-up, is critical to the proper management of cancer patient. A PET specialist is different from a conventional radiologist, and proper interpretation of a PET image is different from a radiological film reading. PET specialists have to integrate the clinical, laboratory, pathophysiological, and even biochemical understandings on a specific disease and related disease progress. With the new development of molecular imaging agents and hybrid imaging modalities including PET/CT or PET/MRI, interactive multidisciplinary communications and international collaborations become more and more important [44, 45]. In the future, interactive communication methods include, but not limited to regular specialist attendance at team meetings, telephone discussions but also shared electric archives and massive open online course (MOOC). We assume that when cloud-based medical practice is applied for the future clinical practice, interactive communication will be even more important and more related to the better patient management.

22.9 Conclusions

Interactive communication is feedback and teamwork. Awareness of the impact of interactive communication between PET specialists and oncologists is critical to the proper management of cancer patient.

Open Access This chapter is distributed under the terms of the Creative Commons Attribution-Noncommercial 2.5 License (<http://creativecommons.org/licenses/by-nc/2.5/>) which permits any noncommercial use, distribution, and reproduction in any medium, provided the original author(s) and source are credited.

The images or other third party material in this chapter are included in the work's Creative Commons license, unless indicated otherwise in the credit line; if such material is not included in the work's Creative Commons license and the respective action is not permitted by statutory regulation, users will need to obtain permission from the license holder to duplicate, adapt or reproduce the material.

References

1. *National Survey Report conducted by Chinese Society of Nuclear Medicine*. Chin J Nucl Med. 2014; 34(5): pp. 389–391.
2. Bar-Shalom R, et al. Clinical performance of PET/CT in evaluation of cancer: additional value for diagnostic Imaging and patient management. J Nucl Med. 2003;44(8):1200–9.
3. Kruse V, Van Belle S, Cocquyt V. Imaging requirements for personalized medicine: the oncologists point of view. Curr Pharm Des. 2014;20(14):2234–49.
4. Gambhir SS. Molecular imaging of cancer with positron emission tomography. Nat Rev Cancer. 2002;2(9):683–93.
5. Pieterman RM, et al. Preoperative staging of non-small-cell lung cancer with positron-emission tomography. N Engl J Med. 2000;343(4):254–61.
6. Riedl CC, et al. Retrospective analysis of 18F-FDG PET/CT for staging asymptomatic breast cancer patients younger than 40 years. J Nucl Med. 2014;55(10):1578–83.
7. Wahl RL, et al. From RECIST to PERCIST: evolving considerations for PET response criteria in solid tumors. J Nucl Med. 2009;50 Suppl 1:122S–50.
8. Bradley J, et al. Impact of FDG-PET on radiation therapy volume delineation in non-small-cell lung cancer. Int J Radiat Oncol Biol Phys. 2004;59(1):78–86.
9. Avril NE, .Weber WA. Monitoring response to treatment in patients utilizing PET. Radiol Clin North Am. 2005; 43(1): 189 – +.
10. Afshar-Oromieh A, et al. Comparison of PET imaging with a Ga-68-labelled PSMA ligand and F-18-choline-based PET/CT for the diagnosis of recurrent prostate cancer. Eur J Nucl Med Mol Imaging. 2014;41(1):11–20.
11. Marcus C, et al. F-18-FDG PET/CT and lung cancer: value of fourth and subsequent posttherapy follow-up scans for patient management. J Nucl Med. 2015;56(2):204–8.
12. Board CNE. Types of oncologists, 2013; Available from: <http://www.cancer.net/navigating-cancer-care/cancer-basics/cancer-care-team/types-oncologists>
13. Jadvar H. Prostate cancer: PET with F-18-FDG, F-18- or C-11-Acetate, and F-18- or C-11-Choline. J Nucl Med. 2011;52(1):81–9.
14. Nam EJ, et al. Diagnosis and staging of primary ovarian cancer: correlation between PET/CT, Doppler US, and CT or MRI. Gynecol Oncol. 2010;116(3):389–94.
15. Sosna J, et al. Blind spots at oncological CT: lessons learned from PET/CT. Cancer Imaging. 2012;12:259–68.
16. Lan BY, Kwee SA, Wong LL. Positron emission tomography in hepatobiliary and pancreatic malignancies: a review. Am J Surg. 2012;204(2):232–41.
17. Fact sheet N°297. World Health Organization. February 2014, <http://www.who.int/mediacentre/factsheets/fs297/en/>
18. Meller J, Sahlmann CO, Scheel AK. F-18-FDG PET and PET/CT in fever of unknown origin. J Nucl Med. 2007;48(1):35–45.
19. Hernandez-Maraver D, et al. A prospective study comparing CT, PET and PET/CT for pre-treatment clinical staging in Non-Hodgkin's and Hodgkin's lymphoma. Blood. 2009;114(22):1508.
20. Ishimori T, Patel PV, Wahl RL. Detection of unexpected additional primary malignancies with PET/CT. J Nucl Med. 2005;46(5):752–7.
21. Seevaratnam R, et al. How useful is preoperative imaging for tumor, node, metastasis (TNM) staging of gastric cancer? A meta-analysis. Gastric Cancer. 2012;15 Suppl 1:S3–18.
22. Fischer B, et al. Preoperative staging of lung cancer with combined PET-CT. N Engl J Med. 2009;361(1):32–9.
23. Lardinois D, et al. Staging of non-small-cell lung cancer with integrated positron-emission tomography and computed tomography. N Engl J Med. 2003;348(25):2500–7.
24. Hanna GG, et al. Conventional 3D staging PET/CT in CT simulation for lung cancer: impact of rigid and deformable target volume alignments for radiotherapy treatment planning. Br J Radiol. 2011;84(1006):919–29.

25. Antoch G, et al. Whole-body dual-modality PET/CT and whole-body MRI for tumor staging in oncology. *JAMA*. 2003;290(24):3199–206.
26. Antoch G, et al. Accuracy of whole-body dual-modality fluorine-18-2-fluoro-2-deoxy-D-glucose positron emission tomography and computed tomography (FDG-PET/CT) for tumor staging in solid tumors: comparison with CT and PET. *J Clin Oncol*. 2004;22(21):4357–68.
27. Skougaard K, et al. CT versus FDG-PET/CT response evaluation in patients with metastatic colorectal cancer treated with irinotecan and cetuximab. *Cancer Med*. 2014;3(5):1294–301.
28. Venook AP. Epidermal growth factor receptor-targeted treatment for advanced colorectal carcinoma. *Cancer*. 2005;103(12):2435–46.
29. Lenz HJ, et al. Multicenter phase II and translational study of cetuximab in metastatic colorectal carcinoma refractory to irinotecan, oxaliplatin, and fluoropyrimidines. *J Clin Oncol*. 2006;24(30):4914–21.
30. Contractor KB, Aboagye EO. Monitoring predominantly cytostatic treatment response with 18F-FDG PET. *J Nucl Med*. 2009;50 Suppl 1:97S–105.
31. Kuwatani M, et al. Modalities for evaluating chemotherapeutic efficacy and survival time in patients with advanced pancreatic cancer: comparison between FDG-PET, CT, and serum tumor markers. *Intern Med*. 2009;48(11):867–75.
32. Siegel R, et al. Cancer treatment and survivorship statistics, 2012. *CA Cancer J Clin*. 2012;62(4):220–41.
33. Israel O, Kuten A. Early detection of cancer recurrence: 18F-FDG PET/CT can make a difference in diagnosis and patient care. *J Nucl Med*. 2007;48 Suppl 1:28S–35.
34. Antoniou AJ, et al. Follow-up or surveillance F-18-FDG PET/CT and survival outcome in lung cancer patients. *J Nucl Med*. 2014;55(7):1062–8.
35. Keidar Z, et al. PET/CT using F-18-FDG in suspected lung cancer recurrence: diagnostic value and impact on patient management. *J Nucl Med*. 2004;45(10):1640–6.
36. Nanni C, et al. 18F-FACBC compared with 11C-Choline PET/CT in patients with biochemical relapse after radical prostatectomy: a prospective study in 28 patients. *Clin Genitourinary Cancer*. 2014;12(2):106–10.
37. Cheung TT, et al. C-11-Acetate and F-18-FDG PET/CT for clinical staging and selection of patients with hepatocellular carcinoma for liver transplantation on the basis of Milan criteria: surgeon's perspective. *J Nucl Med*. 2013;54(2):192–200.
38. Kashyap R, et al. Role of N-13 ammonia PET/CT in diagnosing pancreatic necrosis in patients with acute pancreatitis as compared to contrast enhanced CT – results of a pilot study. *Pancreatology*. 2014;14(3):154–8.
39. Cherry SR, et al. MicroPET: a high resolution PET scanner for imaging small animals. *IEEE Trans Nucl Sci*. 1997;44(3):1161–6.
40. Tai YC, et al. Performance evaluation of the microPET focus: a third-generation microPET scanner dedicated to animal imaging. *J Nucl Med*. 2005;46(3):455–63.
41. Chang JM, et al. False positive and false negative FDG-PET scans in various thoracic diseases. *Korean J Radiol*. 2006;7(1):57–69.
42. Rosenbaum SJ, et al. False-positive FDG PET uptake – the role of PET/CT. *Eur Radiol*. 2006;16(5):1054–65.
43. Chung JH, et al. Overexpression of Glut1 in lymphoid follicles correlates with false-positive F-18-FDG PET results in lung cancer staging. *J Nucl Med*. 2004;45(6):999–1003.
44. Soderlund TA et al. Beyond 18F-FDG: characterization of PET/CT and PET/MR scanners for a comprehensive set of positron emitters of growing application – 18F, 11C, 89Zr, 124I, 68Ga and 90Y. *J Nucl Med*, 2015.
45. Zhou J, et al. Fluorine-18-labeled Gd³⁺/Yb³⁺/Er³⁺ co-doped NaYF₄ nanophosphors for multimodality PET/MR/UCL imaging. *Biomaterials*. 2011;32(4):1148–56.

Chapter 23

Clinical Efficacy of PET/CT Using ^{68}Ga -DOTATOC for Diagnostic Imaging

Yuji Nakamoto, Takayoshi Ishimori, and Kaori Togashi

Abstract Positron emission tomography/computed tomography (PET/CT) using ^{68}Ga -labelled DOTA⁰-Tyr³ octreotide (DOTATOC) is one of the diagnostic imaging tools in somatostatin receptor scintigraphy. There have been many studies demonstrating the clinical usefulness of this diagnostic imaging method, especially for detecting neuroendocrine tumors (NETs). It often yields clinically relevant information for determining therapeutic management in NET patients. However, we have found that the usefulness of the information provided depends on the clinical situation; for example, it was considered especially helpful when recurrence/metastasis was suspected after surgery for histopathologically proven NET. In addition to NETs, DOTATOC PET/CT sometimes provides useful information in patients with tumor-induced osteomalacia (TIO), in which fibroblast growth factor 23 produced by a mesenchymal tumor causes hypophosphatemia, resulting in osteomalacia. As these mesenchymal tumors frequently express somatostatin receptors, DOTATOC PET/CT would be expected to detect causative lesions in TIO. Furthermore, many renal cell carcinomas (RCC) are not FDG avid. DOTATOC PET/CT could be helpful for detecting unexpected lesions when recurrence or metastasis is suspected after surgery for RCC. DOTATOC PET/CT is also able to reveal additional findings even in sarcoidosis, an inflammatory disease. The clinical value of DOTATOC PET/CT is discussed, based on our clinical experience.

Keywords PET/CT • DOTATOC • Neuroendocrine tumor • Tumor-induced osteomalacia

Y. Nakamoto, M.D., Ph.D. (✉) • T. Ishimori • K. Togashi
Department of Diagnostic Imaging and Nuclear Medicine, Kyoto University Graduate School of Medicine, 54 Shogoinkawahara-cho, Sakyo-Ku, Kyoto 606-8507, Japan
e-mail: ynakamo1@kuhp.kyoto-u.ac.jp

23.1 Current Status of Somatostatin Receptor Scintigraphy in Japan

In diagnostic imaging of cancers, positron emission tomography (PET) using ^{18}F -labeled fluorodeoxyglucose (FDG) has been widely accepted clinically for staging and restaging, monitoring therapy response, and detecting unknown primary sites. However, there are some tumors for which FDG PET/CT does not provide relevant information owing to their insufficient FDG avidity. Such tumors include well-differentiated neuroendocrine tumors (NETs), which often cannot be identified as hypermetabolic areas on FDG PET/CT [1]. A major characteristic of NETs is that they express somatostatin receptors. For scintigraphy targeting such receptors, a radiolabeled octreotide, which has high affinity for somatostatin receptors and is very stable *in vivo*, has been used in Europe and the United States. Compounds labeled with ^{111}In or $^{99\text{m}}\text{Tc}$ are used as tracers for single photon emission computed tomography (SPECT), and tracers labeled with ^{68}Ga are used for PET.

^{111}In -pentetreotide (OctreoScan) is a commercially available radiopharmaceutical. It is routinely used clinically in Europe and the United States. However, it is not currently approved for use in Japan (as of July 2015), although clinical trials were conducted about the year 2000. Patients must travel to Europe to receive this examination or personally arrange importation of this radiopharmaceutical to enable them to undergo scintigraphy in one of several academic institutions. The number of patients with gastroenteropancreatic NETs is relatively small compared with the number with other common cancers, but its incidence has been increasing [2] so that it is becoming a serious issue. In our institution, PET/CT with ^{68}Ga -DOTATOC for somatostatin receptor scintigraphy has performed since 2011. More than 300 patients have had this examination here over the last 4 years.

23.2 Usefulness in NET According to Clinical Situation

There have been many reports demonstrating the clinical usefulness of PET/CT with ^{68}Ga -DOTATOC or other ^{68}Ga -labeled PET tracers in NETs. It has been reported that it is superior to FDG PET/CT in well-differentiated NET and medullary thyroid cancer [3–5] and scintigraphy using ^{111}In -labeled compounds [6]. Its diagnostic accuracy, including sensitivity and specificity, is reasonably high (more than 90 %) according to a few meta-analyses [7, 8]. However, there are some patients with high hormone levels, indicating the presence of NETs, in whom DOTATOC PET/CT reveals no additional information.

We investigated the clinical value of DOTATOC PET/CT in relation to the clinical situation [9]. We divided patients into three groups: groups A, B, and C. In group A, PET/CT was performed after metastatic NET had been confirmed histopathologically, but the primary tumor had not been identified by other conventional imaging modalities. In group B, PET/CT was performed to evaluate suspected

recurrent lesions due to high hormone levels after the patient had undergone curative surgery for histologically proven NET. Conventional imaging had been negative before DOTATOC PET/CT. In group C, NET was suspected based on laboratory data without definitive localization of the primary site by conventional imaging.

In group A, there were 14 patients who were suspected of having a primary NET because of pathologically proven liver metastasis (9 patients), nodal metastasis (3 patients), or bone metastasis (2 patients). In four of the nine patients with liver metastasis, DOTATOC PET/CT demonstrated positive findings, indicating a suspected primary tumor in the duodenum (2 patients), jejunum (1 patient), and pancreatic tail (1 patient) with the maximum standardized uptake value (SUVmax) ranging from 2.8 to 19.7. DOTATOC PET/CT showed no abnormal findings in the remaining five patients. In three patients with nodal metastasis, DOTATOC PET/CT revealed abnormal uptake in the duodenum (1 patient) and jejunum (2 patients). In two patients with bone metastasis, DOTATOC PET/CT was negative in one but showed intense focal uptake in the prostate in the other, suggesting prostate cancer. However, the uptake was found, by biopsy, to be due to benign prostatic hypertrophy. Thus, a final diagnosis of a gastroenteropancreatic NET was obtained in 7 of the 14 patients (50 %).

In group B, seven patients underwent surgery for a NET. Except for one patient with a high insulin level, DOTATOC PET/CT detected ten lesions in six patients with the SUVmax ranging from 7.9 to 70.1. Two patients had histopathological confirmation after surgery, and the remaining four patients were followed up with no surgical treatment. Thus, DOTATOC PET/CT provided additional information in six of seven patients (86 %). PET/CT imaging in a representative patient with nodal metastasis is shown in Fig. 23.1.

In group C, a total of 25 patients with suspected NET due to high hormone levels underwent DOTATOC PET/CT. A pancreatic NET with SUVmax 68.5 was clearly shown by DOTATOC PET/CT in a patient with a suspected ACTH-producing tumor, followed by surgical confirmation. In the remaining 24 patients, DOTATOC

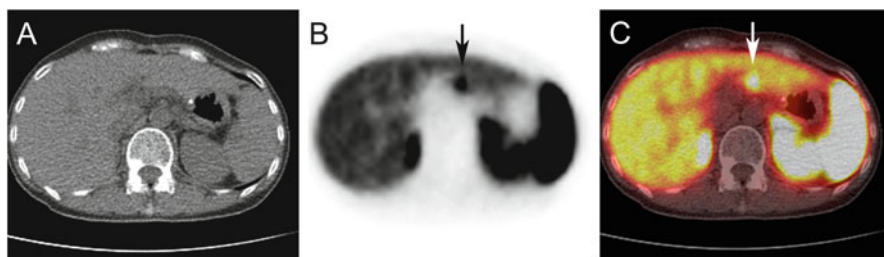


Fig. 23.1 A 51-year-old woman with suspected recurrent gastrinoma. Axial CT (a), DOTATOC PET (b), and fused (c) images are shown. A duodenal gastrinoma was removed by surgery, but recurrence was suspected because of rising serum gastrin levels. Intense focal uptake around the lateral segment of the liver is apparent on the DOTATOC PET and fused images (arrows). A lymph node metastasis was confirmed by surgery

PET/CT did not provide any additional clinically relevant information. The detection rate was significantly lower than in the other groups (Fisher's exact test, $p < 0.01$).

We concluded that DOTATOC PET/CT is useful for detecting NET, especially when recurrence or metastases are suspected because of high hormone levels after surgery for a primary NET and that it is hardly helpful in patients in whom only the hormone levels are high and the tumor has not been localized.

It is reasonable that DOTATOC PET/CT would be expected to yield relevant information when recurrence or metastasis is suspected due to high hormone levels after surgery for a functioning NET, since the pretest probability is high. In the patient shown in Fig. 23.1, a small lymph node was visualized retrospectively on contrast-enhanced CT (figure not shown), but it was difficult to distinguish from a benign inflammatory node on the basis of size. In addition, it would take time to confirm the characteristics during follow-up owing to its slow growth. The high accumulation of DOTATOC in a subcentimeter node is considered a useful finding for raising the suspicion of recurrence or metastasis after surgery for NET. Conversely, among the patients without a history of NET, only in one patient was DOTATOC PET/CT helpful, and it was negative in the remaining 24 patients. Some reasons might be considered. Primary sites may be too small to be detected by imaging modalities. If lesions are extremely small, uptake of DOTATOC could be underestimated because of the partial volume phenomenon. Also, when the primary tumor is located in the upper abdomen or alimentary tract, uptake could easily be influenced by respiratory motion or peristalsis, resulting in underestimation of uptake. In addition, high hormone levels do not always mean the presence of NET because hyperfunctioning can cause high hormone levels, e.g., nesidioblastosis in hyperinsulinemia or G-cell hyperplasia in hypergastrinemia. Furthermore, it has been reported that somatostatin receptor subtypes 2 and 5 are not well expressed in many insulinomas [10]. For these reasons, DOTATOC PET/CT may fail to show the primary tumor.

Peptide receptor radionuclide therapy (PRRT) using ^{177}Lu -labeled or ^{90}Y -labeled octreotide has been used to treat NETs in Europe. To stratify patients according to their expected response to therapy, somatostatin receptor scintigraphy, including DOTATOC PET/CT, can be considered. However, we have no sufficient data so far on this subject because PRRT has not yet been performed in our country.

23.3 Localization of Causative Lesions in Tumor-Induced Osteomalacia

It is known that DOTATOC PET/CT is useful not only in the imaging of NETs but also in other diseases. Tumor-induced osteomalacia (TIO) is considered a suitable target for somatostatin receptor scintigraphy. TIO, which is also known as oncogenic osteomalacia, is a rare paraneoplastic syndrome. Phosphaturic mesenchymal

tumors secrete fibroblast growth factor 23 (FGF-23), causing hypophosphatemia due to suppression of the reabsorption of phosphorus in the proximal renal tubule and activation of vitamin D synthesis. Consequently, these tumors cause osteomalacia. Total resection of this mesenchymal tumor is essential to achieve complete cure, but localization of the causative lesions remains a challenge because they are usually small, slow growing, and are located at peculiar sites. Therefore, somatostatin receptor scintigraphy can be expected to be useful because these tumors often express somatostatin receptors [11].

There have been several studies investigating the potential usefulness of somatostatin receptor scintigraphy for detecting these mesenchymal tumors. As a preliminary evaluation in our institution, DOTATOC PET/CT has been performed for this purpose. We analyzed 14 patients (5 men and 9 women, mean age 46 years) with TIO who underwent DOTATOC PET/CT. All these patients had been suspected of having TIO due to hypophosphatemia (<2.5 mg/dl) and a high serum FGF-23 level (49–1,020 pg/ml). Overall, DOTATOC PET/CT showed 12 sites of abnormal uptake in eight patients. However, three lesions corresponding to bone were found to be fractured or pseudofractured, i.e., false-positive. Therefore, nine lesions in seven patients were finally considered to be the cause of the TIO. These lesions were located in the sphenoid bone, spine, rib, pelvic bone, tibia, and muscles. In the remaining six patients, DOTATOC PET/CT was negative. One patient is shown in Fig. 23.2. The serum FGF-23 levels in seven patients with true-positive DOTATOC PET/CT findings tended to be higher than in patients who had no causative tumor detected, but the difference was not significant. FDG PET/CT revealed only two abnormal foci in this population. Our preliminary data suggest that DOTATOC PET/CT would be a useful noninvasive technique for localizing causative tumors in patients with TIO and that fractures or pseudofractures caused by osteomalacia can be a pitfall in interpreting DOTATOC PET/CT images.

This is one of the hot topics in somatostatin receptor scintigraphy. Chong et al. found that ^{111}In -octreotide SPECT(/CT) was better than FDG PET/CT in detecting primary mesenchymal tumors causing TIO, with a sensitivity of 95 % [12]. Jing et al. showed the clinical value of $^{99\text{m}}\text{Tc}$ -HYNIC-TOC with a sensitivity of 86 % [13]. Other studies have demonstrated 100 % sensitivity of DOTATATE PET/CT in detecting causative lesions, although the number of cases is small [14–16]. In our experience, DOTATOC PET/CT does not always show the causative lesions, but this noninvasive technique may be considered even when TIO is suspected and the results of venous sampling are positive, because unexpected lesions can sometimes be detected by DOTATOC PET/CT.

23.4 Restaging in Renal Cell Carcinoma

Renal cell carcinoma (RCC) may be a target for somatostatin receptor scintigraphy because some recurrent or metastatic lesions from RCC are not FDG avid [17] and it has been reported that OctreoScan shows RCC metastasis [18]. At this time, experience with DOTATOC PET/CT in RCC is limited [19]. We have performed a

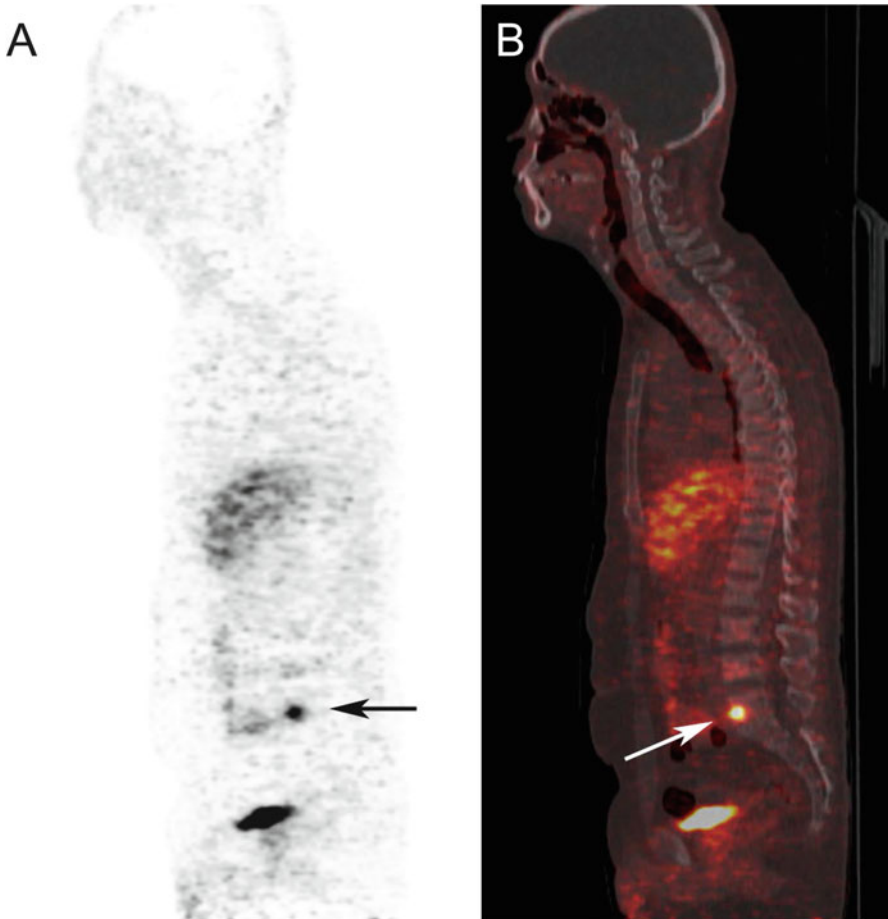


Fig. 23.2 A 54-year-old man with tumor-induced osteomalacia. Sagittal DOTATOC PET (a) and fused (b) images are shown. This patient was suspected of having tumor-induced osteomalacia due to his high FGF-23 level and hypophosphatemia. Intense focal uptake in the lumbar spine is apparent on the DOTATOC PET and fused images (arrows). The lesion was resected, and the patient's phosphorus level returned to normal

preliminary evaluation of the clinical efficacy of DOTATOC PET/CT in patients with suspected recurrent RCC after surgery. Seven consecutive patients who had surgery for histologically proven RCC and who were suspected of having recurrence of RCC underwent DOTATOC PET/CT for restaging. We retrospectively reviewed the PET/CT images and compared available FDG PET/CT findings. In this investigation, there were 18 recurrent or metastatic lesions in seven patients. Of the 18 lesions, 13 in six patients with clear-cell carcinoma were clearly shown on DOTATOC PET/CT, with SUVmax ranging from 2.8 to 23.3 (average 9.7). Excluding 2 of 13 lesions that were not assessed by FDG PET/CT, only three lesions were positive on FDG PET/CT. Four lesions were negative on DOTATOC PET/CT, but positive on FDG PET/CT in a patient with papillary carcinoma.

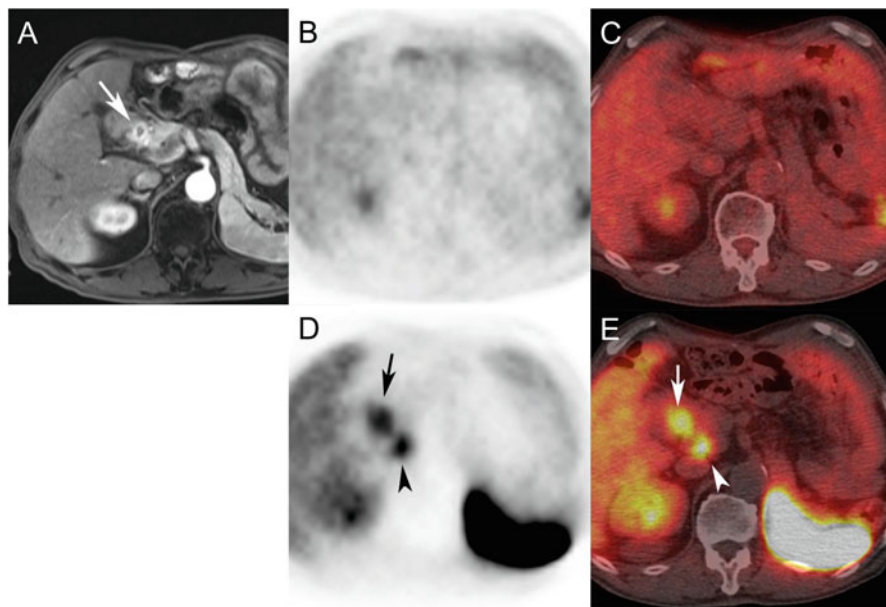


Fig. 23.3 A 76-year-old man with a hypervascular pancreatic tumor. Contrast-enhanced MR (a), FDG PET (b), FDG PET/CT (c), DOTATOC PET (d), and DOTATOC PET/CT (e) images are shown. The contrast-enhanced MR image (a) shows a well-enhanced mass in the pancreatic head (arrow). The FDG PET image (b) shows no abnormal uptake corresponding to this lesion, but the DOTATOC PET (d) and the DOTATOC PET/CT (e) images show DOTATOC accumulation in this tumor (arrows). A pancreatic neuroendocrine tumor and pancreatic metastasis from renal cell carcinoma was suspected. The final diagnosis was metastatic pancreatic tumor from renal cell carcinoma. Physiological uptake in a part of pancreas is also seen on the DOTATOC PET images (arrowheads)

Overall, the sensitivities of DOTATOC PET/CT and FDG PET/CT were 86 % and 67 %, respectively, on a patient basis and 72 % and 56 %, respectively, on a lesion basis, in our population.

A hypervascular tumor seen in the pancreas in a patient with a history of RCC may be difficult to differentiate from pancreatic NET and metastasis from RCC (Fig. 23.3). However, when inconclusive findings are obtained by conventional imaging, DOTATOC PET/CT would be useful for detecting unexpected additional metastatic lesions, just as FDG PET sometimes provides useful information if FDG-avid tumors are present.

23.5 Sarcoidosis

As somatostatin receptors are expressed on activated lymphocytes, it is expected that sarcoidosis, an inflammatory disorder, may also be visualized. The use of somatostatin receptor scintigraphy with ^{111}In -pentetreotide in patients with

sarcoidosis was investigated in one study [20]. The somatostatin receptor imaging was able to demonstrate active granulomatous disease in the patients with sarcoidosis, and pathological uptake of radioactivity in the parotid glands during imaging was correlated with higher serum ACE concentrations. However, the efficacy of somatostatin receptor imaging in sarcoidosis has not yet been established, and there are few articles regarding the clinical utility of DOTATOC PET/CT in sarcoidosis. In our experience, DOTATOC PET/CT reveals a similar or greater number of lesions than a conventional gallium scan. As compared with FDG PET/CT, uptake may be lower in involved nodes, but DOTATOC PET/CT could be useful for evaluating involvement of the myocardium in patients with cardiac sarcoidosis, because physiological uptake in the myocardium can make FDG PET/CT images difficult to evaluate. A representative patient with sarcoidosis is shown in Fig. 23.4.

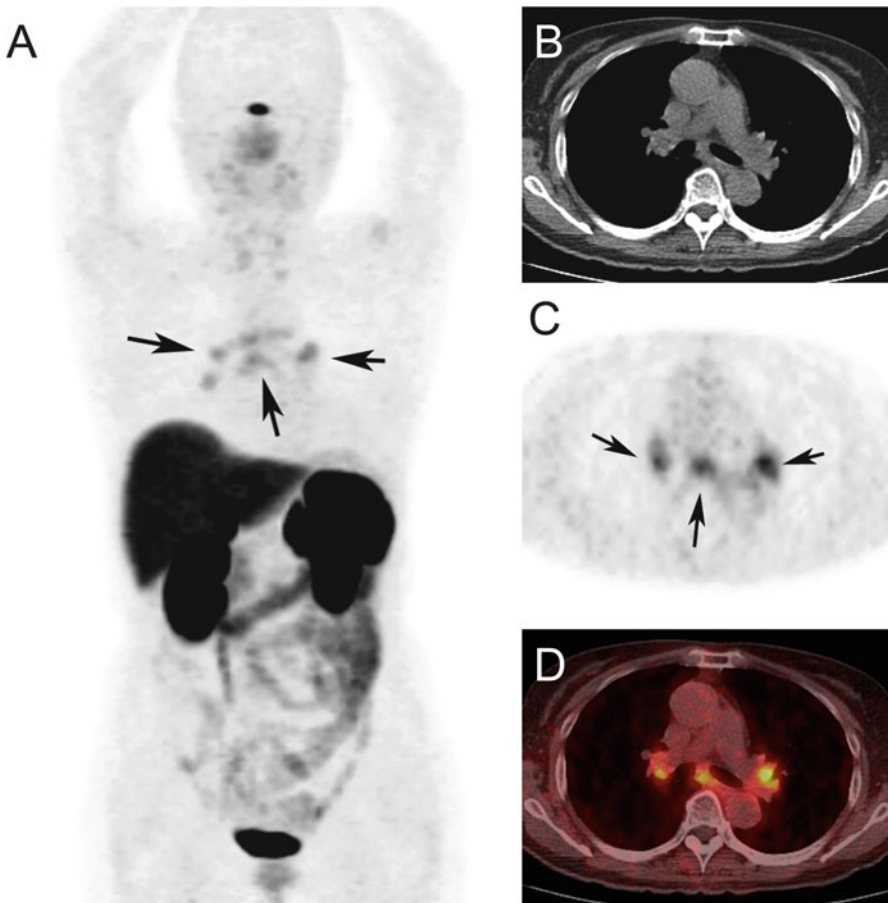


Fig. 23.4 A 65-year-old woman with suspected sarcoidosis. A maximum intensity projection image (a) and axial CT (b), DOTATOC PET (c), and fused (d) images are shown. Moderate to intense uptake of DOTATOC is observed in hilar and mediastinal lymph nodes (arrows)

23.6 Conclusion

DOTATOC PET/CT is a useful imaging modality for detecting NETs, as has been reported in many articles; however, its efficacy depends on the clinical situation. It may be helpful especially when recurrence or metastasis is suspected after surgery of NET, but additional information might not be obtained simply when hormone levels are high. DOTATOC PET/CT is also considered helpful for identifying causative lesions in TIO, although fracture or pseudofracture can be a pitfall. DOTATOC PET/CT could have a clinical impact in restaging of RCC or in detecting involved lesions in sarcoidosis, but further investigations with more patients are required.

Conflict of Interest None.

Open Access This chapter is distributed under the terms of the Creative Commons Attribution-Noncommercial 2.5 License (<http://creativecommons.org/licenses/by-nc/2.5/>) which permits any noncommercial use, distribution, and reproduction in any medium, provided the original author(s) and source are credited.

The images or other third party material in this chapter are included in the work's Creative Commons license, unless indicated otherwise in the credit line; if such material is not included in the work's Creative Commons license and the respective action is not permitted by statutory regulation, users will need to obtain permission from the license holder to duplicate, adapt or reproduce the material.

References

1. van Essen M, Sundin A, Krenning EP, Kwekkeboom DJ. Neuroendocrine tumours: the role of imaging for diagnosis and therapy. *Nat Rev Endocrinol*. 2014;10:102–14.
2. Ito T, Igarashi H, Nakamura K, Sasano H, Okusaka T, Takano K, et al. Epidemiological trends of pancreatic and gastrointestinal neuroendocrine tumors in Japan: a nationwide survey analysis. *J Gastroenterol*. 2015;50:58–64.
3. Kayani I, Bomanji JB, Groves A, Conway G, Gacinovic S, Win T, et al. Functional imaging of neuroendocrine tumors with combined PET/CT using ^{68}Ga -DOTATATE (DOTA-DPhe1, Tyr3-octreotate) and ^{18}F -FDG. *Cancer*. 2008;112:2447–55.
4. Kayani I, Conry BG, Groves AM, Win T, Dickson J, Caplin M, et al. A comparison of ^{68}Ga -DOTATATE and ^{18}F -FDG PET/CT in pulmonary neuroendocrine tumors. *J Nucl Med*. 2009;50:1927–32.
5. Conry BG, Papanthasiou ND, Prakash V, Kayani I, Caplin M, Mahmood S, et al. Comparison of (^{68}Ga)-DOTATATE and (^{18}F)-fluorodeoxyglucose PET/CT in the detection of recurrent medullary thyroid carcinoma. *Eur J Nucl Med Mol Imaging*. 2010;37:49–57.
6. Buchmann I, Henze M, Engelbrecht S, et al. Comparison of ^{68}Ga -DOTATOC PET and ^{111}In -DTPAOC (Octreoscan) SPECT in patients with neuroendocrine tumours. *Eur J Nucl Med Mol Imaging*. 2007;34:1617–26.
7. Treglia G, Castaldi P, Rindi G, Eisenhut M, Runz A, Schäfer M, et al. Diagnostic performance of Gallium-68 somatostatin receptor PET and PET/CT in patients with thoracic and gastroenteropancreatic neuroendocrine tumours: a meta-analysis. *Endocrine*. 2012;42:80–7.

8. Geijer H, Breimer LH. Somatostatin receptor PET/CT in neuroendocrine tumours: update on systematic review and meta-analysis. *Eur J Nucl Med Mol Imaging*. 2013;40:1770–80.
9. Nakamoto Y, Sano K, Ishimori T, Ueda M, Temma T, Saji H, et al. Additional information gained by positron emission tomography with (68)Ga-DOTATOC for suspected unknown primary or recurrent neuroendocrine tumors. *Ann Nucl Med*. 2015;29:512–8.
10. Portela-Gomes GM, Stridsberg M, Grimelius L, Rorstad O, Janson ET. Differential expression of the five somatostatin receptor subtypes in human benign and malignant insulinomas – predominance of receptor subtype 4. *Endocr Pathol*. 2007;18:79–85.
11. Houang M, Clarkson A, Sioson L, Elston MS, Clifton-Bligh RJ, Dray M, et al. Phosphaturic mesenchymal tumors show positive staining for somatostatin receptor 2A (SSTR2A). *Hum Pathol*. 2013;44:2711–8.
12. Chong WH, Andreopoulou P, Chen CC, Reynolds J, Guthrie L, Kelly M, et al. Tumor localization and biochemical response to cure in tumor-induced osteomalacia. *J Bone Miner Res*. 2013;28:1386–98.
13. Jing H, Li F, Zhuang H, Wang Z, Tian J, Xing X, et al. Effective detection of the tumors causing osteomalacia using [Tc-99m]-HYNIC-octreotide (99mTc-HYNIC-TOC) whole body scan. *Eur J Radiol*. 2013;82:2028–34.
14. Clifton-Bligh RJ, Hofman MS, Duncan E, Sim IeW, Darnell D, Clarkson A, et al. Improving diagnosis of tumor-induced osteomalacia with Gallium-68 DOTATATE PET/CT. *J Clin Endocrinol Metab*. 2013;98:687–94.
15. Breer S, Brunkhorst T, Beil FT, Peldschus K, Heiland M, Klutmann S, et al. 68Ga DOTA-TATE PET/CT allows tumor localization in patients with tumor-induced osteomalacia but negative 111In-octreotide SPECT/CT. *Bone*. 2014;64:222–7.
16. Jadhav S, Kasaliwal R, Lele V, Rangarajan V, Chandra P, Shah H, et al. Functional imaging in primary tumour-induced osteomalacia: relative performance of FDG PET/CT vs somatostatin receptor-based functional scans: a series of nine patients. *Clin Endocrinol (Oxf)*. 2014;81:31–7.
17. Nakatani K, Nakamoto Y, Saga T, Higashi T, Togashi K. The potential clinical value of FDG-PET for recurrent renal cell carcinoma. *Eur J Radiol*. 2011;79:29–35.
18. Edgren M, Westlin JE, Kälkner KM, Sundin A, Nilsson S. [111In-DTPA-D-Phe1]-octreotide scintigraphy in the management of patients with advanced renal cell carcinoma. *Cancer Biother Radiopharm*. 1999;14:59–64.
19. Peter L, Sanger J, Hommann M, Baum RP, Kaemmerer D. Molecular imaging of late somatostatin receptor-positive metastases of renal cell carcinoma in the pancreas by 68Ga DOTATOC PET/CT: a rare differential diagnosis to multiple primary pancreatic neuroendocrine tumors. *Clin Nucl Med*. 2014;39:713–6.
20. Kwekkeboom DJ, Krenning EP, Kho GS, Breeman WA, Van Hagen PM. Somatostatin receptor imaging in patients with sarcoidosis. *Eur J Nucl Med*. 1998;25:1284–92.

Chapter 24

Correlation of 4'-[methyl-¹¹C]-Thiothymidine Uptake with Ki-67 Immunohistochemistry in Patients with Newly Diagnosed and Recurrent Gliomas

Yuka Yamamoto and Yoshihiro Nishiyama

Abstract Purpose: 4'-[methyl-¹¹C]-thiothymidine (4DST) has been developed as an in vivo cell proliferation marker based on the DNA incorporation method. We evaluated 4DST uptake on PET in patients with newly diagnosed and recurrent gliomas and correlated the results with proliferative activity.

Methods: 4DST PET was investigated in 32 patients, including 21 with newly diagnosed gliomas and 11 with recurrent gliomas. PET imaging was performed at 15 min after 4DST injection. The standardized uptake value (SUV) was determined by region-of-interest analysis. The maximal SUV for tumor (T) and the mean SUV for contralateral normal brain tissue (N) were calculated and T/N ratio was determined. Proliferative activity as indicated by the Ki-67 index was estimated in tissue specimens.

Results: The sensitivity of 4DST PET for the detection of newly diagnosed and recurrent gliomas was 86 % and 100 %, respectively. In newly diagnosed gliomas, there was a weak correlation between T/N ratio and Ki-67 index ($r = 0.45$; $p < 0.05$). In recurrent gliomas, there was no significant difference between T/N ratio and Ki-67 index.

Conclusion: In newly diagnosed gliomas, 4DST PET seems to be useful in the noninvasive assessment of proliferation.

Keywords ¹¹C-4DST • PET • Glioma • Proliferation

Y. Yamamoto (✉) • Y. Nishiyama

Department of Radiology, Faculty of Medicine, Kagawa University, 1750-1 Ikenobe, Miki-cho, Kita-gun, Kagawa 761-0793, Japan

e-mail: yuka@kms.ac.jp

24.1 Introduction

Markers of proliferative activity are essential for individualized patient therapy and management of brain gliomas [1]. Because tissue sampling is often obtained by stereotactic biopsy and, therefore, represents only a small part of the primary tumor, there is a probability of true malignant potential being underestimated [2]. Thus, noninvasive imaging-based technology for the detection of malignant progression is required to select the best possible treatment regimen.

Positron emission tomography (PET) is now an indispensable modality for assessment of various tumors. The radiotracer 3'-deoxy-3'-[¹⁸F]fluorothymidine (FLT) has been investigated as a promising PET tracer for evaluating tumor proliferating activity in brain tumors [3–5]. A theoretic limitation of FLT as a radiotracer for the salvage pathway of DNA synthesis is that it is not incorporated into DNA because of the lack of a 3'-hydroxyl [6].

Toyohara et al. developed 4'-thiothymidine labeled with ¹¹C at the methyl group (4'-[methyl-¹¹C]-thiothymidine [4DST]), as a new candidate for cell proliferation imaging that is resistant to degradation by thymidine phosphorylase and is incorporated into DNA [7, 8]. A ¹¹C-4DST PET pilot study of 6 patients with various brain tumors showed that ¹¹C-4DST PET is feasible for brain tumor imaging and can be performed with acceptable dosimetry and pharmacologic safety at a suitable dose for adequate imaging [9]. In a mixed population of patients with newly diagnosed and recurrent gliomas, Toyota et al. has recently demonstrated that 4DST PET is feasible for evaluating cell proliferation [10]. These results indicate that 4DST has great potential for imaging cell proliferation.

The purpose of this study was to evaluate 4DST uptake in patients with newly diagnosed and recurrent gliomas and to correlate the results with proliferative activity as indicated by the Ki-67 index.

24.2 Materials and Methods

24.2.1 Patients

A total of 32 patients (15 men, 17 women) with brain gliomas who underwent 4DST PET examination were selected. Of the patients, 21 had newly diagnosed gliomas and 11 presented with recurrent gliomas that had been treated with surgery, chemotherapy and radiotherapy previously.

Pathologic diagnosis had been obtained by stereotactic biopsy or open surgery. Grading of the tumor was performed according to the World Health Organization (WHO) classification for neuroepithelial tumors [11]. Distribution of tumor grades according to WHO classification was as follows: grade II ($n = 7$), grade III ($n = 9$), and grade IV ($n = 16$).

24.2.2 4DST Synthesis and PET Imaging

The radiotracer 4DST was produced using an automated synthesis system with HM-18 cyclotron (QUPID; Sumitomo Heavy Industries Ltd, Tokyo, Japan). The 4DST was synthesized using the method described by Toyohara et al. [9].

All acquisitions were performed using a Biograph mCT 64-slice PET/CT scanner (Siemens Medical Solutions USA Inc., Knoxville, TN, USA). Data acquisition began with CT at the following settings: no contrast agent, 120 kV, 192 mA, 1.0-s tube rotation time, 3-mm slice thickness, 3-mm increments, and pitch 0.55. PET emission scanning of the head region with a 15-min acquisition of one bed position was performed 15 min after intravenous injection of 4DST (6 MBq/kg). The PET data were acquired in three-dimensional mode and were reconstructed by the baseline ordered-subset expectation maximization (OSEM) bases, with incorporating correction with point spread-function and time-of-flight model (5 iterations, 21 subsets).

24.2.3 Data Analysis

Visual image analysis was performed by an experienced nuclear physician. Tumor lesions were identified as areas of focally increased uptake, exceeding that of normal brain background.

Semiquantitative analysis was performed using the standardized uptake value (SUV). The region of interest (ROI) was placed over the entire tumor using the transverse PET image. For the reference tissue, a circular ROI of 15 × 15 mm was manually placed on the uninvolved contralateral hemisphere in the same plane that showed maximum 4DST tumor uptake. Radioactivity concentration values measured in the ROI were normalized to injected dose per patient's body weight by calculation of SUV. The maximal SUV for tumor and the mean SUV for reference tissue were calculated. Tumor-to-contralateral normal brain tissue (T/N) ratio was determined by dividing the tumor SUV by that of the contralateral hemisphere.

24.2.4 Ki-67 Immunohistochemistry

Formalin-fixed, paraffin-embedded sections of resected specimens from brain tumor were made for immunohistochemical staining. The Ki-67 index was estimated as the percentage of Ki-67-positive cell nuclei per 500–1,000 cells in the region of the tumor with the greatest density of staining.

24.2.5 Statistical Analysis

All semiquantitative data were expressed as mean \pm SD. The Ki-67 index and the T/N ratio were compared using linear regression analysis. Differences were considered statistically significant at $p < 0.05$.

24.3 Results

24.3.1 4DST Uptake

In newly diagnosed gliomas, 4DST PET detected 3 of 7 grade II gliomas, all 6 grade III gliomas, and all 8 grade IV gliomas. In recurrent gliomas, 4DST PET detected all 3 grade III gliomas and all 8 grade IV gliomas. Although 4DST PET in newly diagnosed gliomas showed a slightly lower detection rate than that in recurrent gliomas (86 % vs. 100 %), the difference was not statistically significant.

24.3.2 4DST Uptake and Ki-67 Immunohistochemistry

In newly diagnosed gliomas, linear regression analysis indicated a weak correlation between T/N ratio and the Ki-67 index ($r = 0.45$, $p < 0.05$; Fig. 24.1a). In recurrent gliomas, there was no significant difference between T/N ratio and the Ki-67 index ($r = 0.31$, $p = 0.36$; Fig. 24.1b).

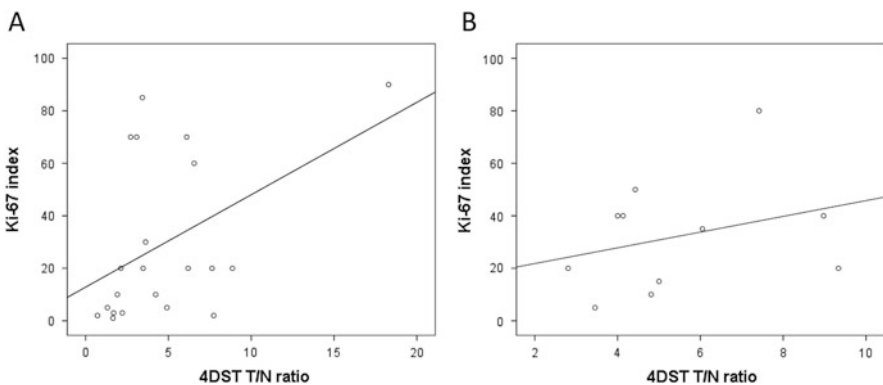


Fig. 24.1 Linear regression analysis demonstrates a weak correlation between 4DST T/N ratio and proliferative activity (Ki-67 index) in newly diagnosed gliomas ($r = 0.45$, $p < 0.05$) (A). There was no significant correlation between 4DST T/N ratio and proliferative activity (Ki-67 index) in recurrent gliomas ($r = 0.31$, $p = 0.36$) (B)

24.4 Discussion

In the present study, we evaluated 4DST uptake in patients with newly diagnosed and recurrent gliomas. 4DST PET was feasible for imaging both newly diagnosed and recurrent gliomas. 4DST PET was found to be useful in the assessment of tumor proliferation in newly diagnosed gliomas.

Increased cell proliferation and DNA replication is a characteristic of malignant transformation [12]. The assessment of cellular proliferation rate by means of PET is useful as a noninvasive clinical approach. In a previous study, an initial clinical trial in only 6 patients with brain tumor was indicated that 4DST PET was feasible for imaging brain tumors [9]. Toyota et al. evaluated 4DST uptake and proliferative activity in 20 patients with gliomas, including 11 recurrent gliomas [10]. They showed a weak correlation between 4DST T/N ratio and Ki-67 index [10]. The present study also showed a weak correlation between 4DST T/N ratio and Ki-67 index in newly diagnosed gliomas. Minamimoto et al. evaluated 4DST uptake and Ki-67 index in patients with non-small cell lung cancer [13]. They showed a significant correlation between 4DST maximal SUV and Ki-67 index [13]. However, Ito et al. showed no significant correlation between 4DST maximal SUV and Ki-67 index in head and neck squamous cell carcinoma [14]. One possible reason for Ito et al.'s findings may be that the Ki-67 index was mainly obtained from biopsy specimens and not from resected specimens.

The present study showed no significant correlation between 4DST T/N ratio and Ki-67 index in recurrent gliomas. Eleven patients with recurrent gliomas in the present study had received chemoradiotherapy before the PET study. Radiation and chemoradiotherapy, used as an adjuvant therapy of gliomas, can cause loosening of endothelial tight junctions, vascular leakage, or endothelial cell death and increase vascular permeability [15]. Radiation could also act to increase vascular permeability not only in the blood-brain barrier (BBB) but also in the blood-tumor barrier (BTB) [15]. We suspect that in recurrent gliomas, breakdown of BBB and BTB contributes to the degree of 4DST uptake in addition to increased proliferation. Furthermore, there is biological difference between newly diagnosed and recurrent gliomas. In recurrent gliomas, recurrent tumor and treatment-induced necrosis frequently coexist.

Because the most proliferating part of the tumor is mainly responsible for tumor progression, 4DST analysis enables a more precise estimation of the malignancy. More important indication is the possibility that the cell proliferation imaging could be used for early evaluation of treatment effects. In the report by Toyohara et al., although ¹¹C-methionine PET detected all the contrast-enhanced lesions visualized with MRI, a clinically stable tumor with contrast enhancement was not detected with 4DST [9]. The role of 4DST in therapy monitoring has not been evaluated so far. Further prospective studies involving a larger number of patients in a variety of tumor types are required to determine the clinical usefulness of 4DST PET for early evaluation of treatment response.

24.5 Conclusion

4DST PET was feasible for imaging both newly diagnosed and recurrent gliomas. 4DST PET seems to be useful in assessment of noninvasive tumor proliferation in newly diagnosed gliomas.

Open Access This chapter is distributed under the terms of the Creative Commons Attribution-Noncommercial 2.5 License (<http://creativecommons.org/licenses/by-nc/2.5/>) which permits any noncommercial use, distribution, and reproduction in any medium, provided the original author(s) and source are credited.

The images or other third party material in this chapter are included in the work's Creative Commons license, unless indicated otherwise in the credit line; if such material is not included in the work's Creative Commons license and the respective action is not permitted by statutory regulation, users will need to obtain permission from the license holder to duplicate, adapt or reproduce the material.

References

1. DeAngelis LM. Brain tumors. *N Engl J Med*. 2001;344:114–23.
2. Ceysens S, Van Laere K, de Groot T, Goffin J, Bormans G, Mortelmans L. [¹¹C]methionine PET, histopathology, and survival in primary brain tumors and recurrence. *AJNR Am J Neuroradiol*. 2006;27:1432–7.
3. Hatakeyama T, Kawai N, Nishiyama Y, et al. ¹¹C-methionine (MET) and ¹⁸F-fluorothymidine (FLT) PET in patients with newly diagnosed glioma. *Eur J Nucl Med Mol Imaging*. 2008;35:2009–17.
4. Jacobs AH, Thomas A, Kracht LW, et al. ¹⁸F-fluoro-L-thymidine and ¹¹C-methylmethionine as markers of increased transport and proliferation in brain tumors. *J Nucl Med*. 2005;46:1948–58.
5. Ullrich R, Backes H, Li H, et al. Glioma proliferation as assessed by 3'-fluoro-3'-deoxy-1-thymidine positron emission tomography in patients with newly diagnosed high-grade glioma. *Clin Cancer Res*. 2008;14:2049–55.
6. Rasey JS, Grierson JR, Wiens LW, et al. Validation of FLT uptake as a measure of thymidine kinase-1 activity in A549 carcinoma cells. *J Nucl Med*. 2002;43:1210–7.
7. Toyohara J, Kumata K, Fukushi K, Irie T, Suzuki K. Evaluation of [methyl-¹⁴C]4-thiothymidine for in vivo DNA synthesis imaging. *J Nucl Med*. 2006;47:1717–22.
8. Toyohara J, Okada M, Toramatsu C, Suzuki K, Irie T. Feasibility studies of 4'-[methyl-¹¹C]thiothymidine as a tumor proliferation imaging agent in mice. *Nucl Med Biol*. 2008;35:67–74.
9. Toyohara J, Nariai T, Sakata M, et al. Whole-body distribution and brain tumor imaging with ¹¹C-4DST: a pilot study. *J Nucl Med*. 2011;52:1322–8.
10. Toyota Y, Miyake K, Kawai N, et al. Comparison of 4'-[methyl-¹¹C]thiothymidine (11C-4DST) and 3'-deoxy-3'-[¹⁸F]fluorothymidine (18F-FLT) PET/CT in human brain glioma imaging. *EJNMMI Res*. 2015;5:7.
11. Louis DN, Ohgaki H, Wiestler OD, et al. The 2007 WHO classification of tumours of the central nervous system. *Acta Neuropathol*. 2007;114:97–109.
12. la Fougère C, Suchorska B, Bartenstein P, Kreth FW, Tonn JC. Molecular imaging of gliomas with PET: opportunities and limitations. *Neuro Oncol*. 2011;13:806–19.
13. Minamimoto R, Toyohara J, Seike A, et al. 4'-[Methyl-¹¹C]-thiothymidine PET/CT for proliferation imaging in non-small cell lung cancer. *J Nucl Med*. 2012;53:199–206.
14. Ito K, Yokoyama J, Miyata Y, et al. Volumetric comparison of positron emission tomography/computed tomography using 4'-[methyl-¹¹C]-thiothymidine with 2-deoxy-2-¹⁸F-fluoro-D-glucose in patients with advanced head and neck squamous cell carcinoma. *Nucl Med Commun*. 2015;36:219–25.
15. Cao Y, Tsien CI, Shen Z, et al. Use of magnetic resonance imaging to assess blood-brain/blood-gliomas barrier opening during conformal radiotherapy. *J Clin Oncol*. 2005;23:4127–36.

Chapter 25

Impact of Respiratory-Gated FMISO-PET/CT for the Quantitative Evaluation of Hypoxia in Non-small Cell Lung Cancer

Shiro Watanabe, Kenji Hirata, Shozo Okamoto, and Nagara Tamaki

Abstract Hypoxia is present in various solid tumors, including non-small cell lung cancer (NSCLC) and is associated with treatment resistance and poor prognosis. ^{18}F -Fluoromisonidazole (FMISO) is a major PET tracer for hypoxia imaging. Previous studies have evaluated the potential role of FMISO-PET as a prognostic tool and assessed tumor reoxygenation following nonsurgical treatment in NSCLC. However, for cancers located in the thorax or abdomen, the patient's breathing causes motion artifacts and misregistration between PET and CT images. PET/CT with the respiratory-gating technique improves the measurement of lesion uptake and tumor volume. We investigated the usefulness of respiratory gating for FMISO-PET/CT-based quantification of hypoxia. Among the 14 patients examined, hypoxia was observed in three patients with non-gated acquisition and in five patients with respiratory gating. The SUVmax, tumor-to-muscle ratio, tumor-to-blood ratio, and hypoxic volume were statistically significantly higher in respiratory-gated (RG) images than in non-respiratory-gated (NG) images. RG FMISO-PET/CT may be useful for the accurate quantification of hypoxia.

Keywords Non-small cell lung cancer • Hypoxia • FMISO • Respiratory gating

25.1 Background

Lung cancer is one of the most common cancers and is the leading cause of cancer death worldwide. Although survival rates have improved in non-small cell lung cancer (NSCLC), the long-term outcome remains poor compared with other cancers. Locoregional failure is not rare, particularly after chemoradiotherapy, and may be attributed to intrinsic tumor resistance to radiotherapy and/or chemotherapy

S. Watanabe (✉) • K. Hirata • S. Okamoto

Department of Nuclear Medicine, Hokkaido University Graduate School of Medicine, North 15th, West 7th, Kitaku, Sapporo 060-8638, Japan

e-mail: shirow@med.hokudai.ac.jp

N. Tamaki

Department of Nuclear Medicine, Graduate School of Medicine, Hokkaido University, Sapporo, Japan

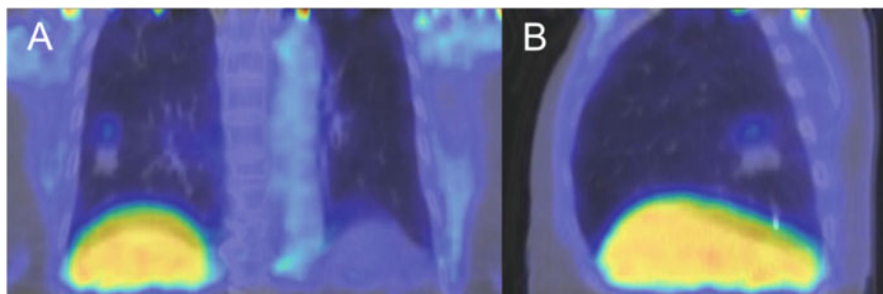


Fig. 25.1 Coronal (a) and sagittal (b) sections of thorax of a NSCLC patient in FMISO-PET/CT. The PET scan shows significant blurring and misregistration of a malignant lung lesion and the liver boundary compared with the CT scan

[1]. Intratumoral hypoxia accelerates radioresistance and chemoresistance, and thus hypoxic tumors require a 2.5–3 times radiotherapy dose to achieve the same cytotoxic effect [2]. Hypoxia may also promote metastatic spread [3].

^{18}F -Fluoromisonidazole (FMISO) is a major PET tracer for hypoxia imaging. The combination of positron emission tomography (PET) and computed tomography (CT) is valuable in cancer diagnosis, follow-up, and treatment management. Previous studies have evaluated the potential role of FMISO-PET as a prognostic tool and in the assessment of the presence of tumor reoxygenation following nonsurgical treatment of NSCLC [1, 4].

However, if the tumor is located in the thorax or abdomen, the patient's breathing causes motion artifacts, resulting in misregistration between PET and CT images (Fig. 25.1) [5]. Because CT is used for attenuation correction of PET images, such misregistration affects image reconstruction. The patient's breathing leads to marked displacement of most of the internal organs, from the apical region of the lungs down to the abdominal organs. Internal organ movement has a degrading effect on image quality and quantitative values in terms of spatial resolution and contrast [6]. Respiratory gating is a technique for improving the measurement of lesion uptake and tumor volume in PET/CT [7]. Motion management is becoming an important issue in both diagnostic and therapeutic applications. A series of studies in ^{18}F -fluorodeoxyglucose PET/CT have shown that respiratory-gated (RG) 4D-PET/CT and breath-holding protocols allow compensation for image degradation and artifacts induced by respiratory movements [6]. In contrast, there has been no study in which RG FMISO-PET/CT was evaluated. We investigated the usefulness of respiratory gating in FMISO-PET/CT-based quantification of hypoxia.

25.2 Materials and Methods

25.2.1 Subjects

We examined 14 patients [8 men, 6 women; median age (range) 78 (50–90) year] with pretreatment stages I–III NSCLC (Table 25.1). None of the patients had ever

Table 25.1 Patient characteristics

Characteristic	Number/value
Male (Female)	8 (6)
Median age (range) [year]	78 (50–90)
Administered FMISO activity [MBq]	397.6 ± 15.7
T stage	
I	8
II	5
III	1
Tumor length (range) [mm]	29.3 (12.0–53.8)

received radiotherapy. The respiratory status of the patients was not considered as an exclusion criterion. All these patients gave their written informed consent to participate in this study. This study was approved by the Institutional Review Board of Hokkaido University.

25.2.2 FMISO-PET/CT Studies

PET images were acquired using a whole-body time-of-flight PET/CT scanner (GEMINI-TF; Philips). We administered 400 MBq of ^{18}F -FMISO intravenously. Four hours after injection, static emission scans with the field of view covering the entire thorax were obtained in the 3D mode. Our protocol included a 4D CT scan and a 30-min list-mode PET acquisition in one bed position centered on the primary tumor. Respiratory signals were detected using a respiratory monitor system (Philips Bellows) with a length sensor in a belt strapped around the patient's upper abdomen.

The PET scanning protocol is shown in Fig. 25.2. To reconstruct RG images, the respiratory cycle was divided into five phases of the same duration. The third phase, which corresponds to expiration, was used for reconstruction. Non-respiratory-gated (NG) images were reconstructed with 6 min of acquisition of PET data (i.e., sub-dataset of 12–18 min were extracted from the complete dataset of 30 min). For all PET image reconstructions, photon attenuation was corrected using 4D CT images. Reconstructions were performed using 3D-RAMLA (ordered subset expectation maximization).

25.2.3 Image Analysis

FMISO uptake 4 h after injection was quantified using (1) standardized uptake values ($\text{SUV} = 1 \text{ g/mL} \times \text{measured radioactivity} \times \text{body weight} / \text{injected radioactivity}$), (2) tumor-to-muscle ratio (TMR), and (3) tumor-to-blood ratio (TBR). Paraspinal muscles were used as the reference muscle. Venous blood was sampled immediately before the PET/CT scanning and counted for radioactivity

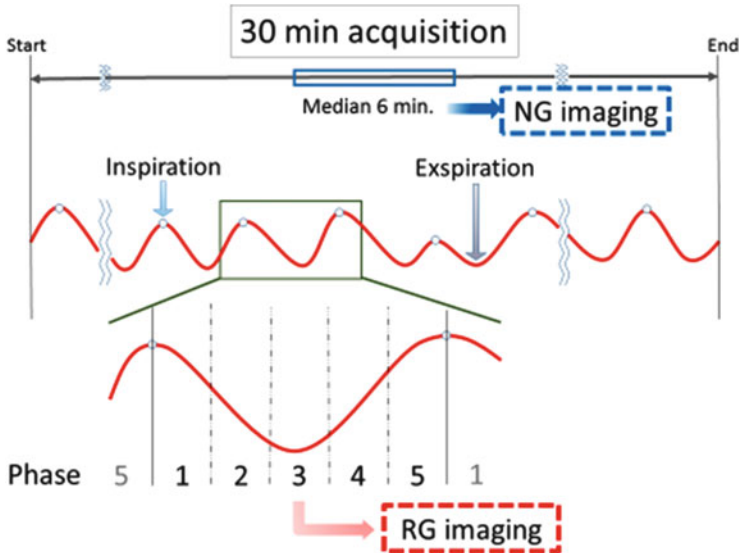


Fig. 25.2 Summary of the PET scan protocol. All the acquisitions lasted 30 min. For respiratory-gated imaging, the third phase, which corresponds to expiration, was used for reconstruction. Non-respiratory-gated images were reconstructed with 6 min of acquired PET data (i.e., 12–18 min)

using a cross-calibrated well counter. We also calculated hypoxic volume (HV) as an area TBR higher than 1.5 [8]. Patients having nonzero HV were considered as having hypoxic tumor. Differences in SUVmax, TMR, TBR, and HV between RG and NG images were statistically analyzed for significance.

25.2.4 Statistical Analysis

All results are expressed here as mean \pm standard deviation (SD). A statistical paired *t*-test was employed to evaluate the statistical significance of the differences in SUVmax, TMR, and TBR between RG and NG. HV was compared between RG and NG images using the Wilcoxon signed-rank test because of the non-normal distribution of HV. P values smaller than 0.05 were considered statistically significant.

25.3 Results and Discussion

In all the 14 patients, the tumor was visually identifiable from its higher signal intensities than the surrounding lung tissues (Figs. 25.3 and 25.4). Quantitatively, SUVmax, TMR, and TBR were all significantly higher on RG images (1.93 ± 1.11 ,

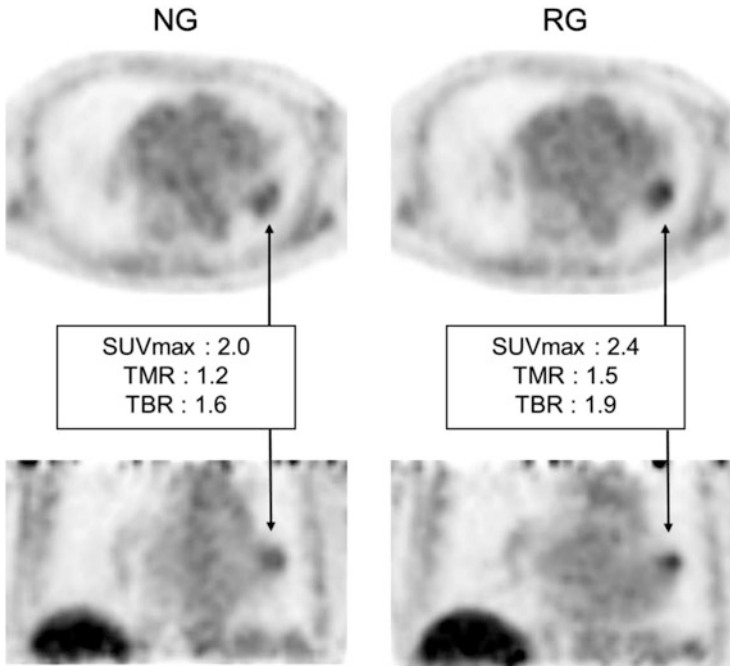


Fig. 25.3 Axial and coronal sections of NG and RG PET images of a patient with a NSCLC lesion in the left lower lobe. In addition to the difference in morphological appearances of the lesion between the NG and RG images, there are considerable increases in SUVmax, TMR, and TBR

1.46 ± 0.78 , and 1.42 ± 0.87 , respectively) than on NG images (2.09 ± 1.11 , 1.61 ± 0.78 , and 1.53 ± 0.87 , respectively) (Table 25.2, Fig. 25.5).

Whereas the NG images showed tumor hypoxia in three patients, the RG images identified tumor hypoxia in two more patients (i.e., a total of 5 patients). In patients with hypoxia, HV on NG images was 12.8 ± 22.6 , whereas that on RG images was 13.2 ± 22.7 , which was significantly higher (Table 25.3).

The results of this study showed significant differences in various quantitative values between RG and NG. Theoretically, RG is less affected by motion artifacts, and thus the images acquired with RG are considered to be more accurate than those with NG. Our data suggest the risk of using non-respiratory gating for FMISO PET in NSCLC, because non-respiratory gating could significantly underestimate tumor hypoxia. Instead, the use of respiratory gating is recommended as a standard technique for treatments targeting a hypoxic region.

The ability to determine the degree and extent of hypoxia in NSCLC is not only important prognostically but also in the selection of candidate patients for hypoxia-modifying treatments. [9] Among different treatments, radiotherapy would most benefit from hypoxia imaging techniques. Radiobiological modeling suggests that hypoxia would have a greater impact on the efficacy of a single-large-fraction treatment than on that of fractionated treatment because of the lack of

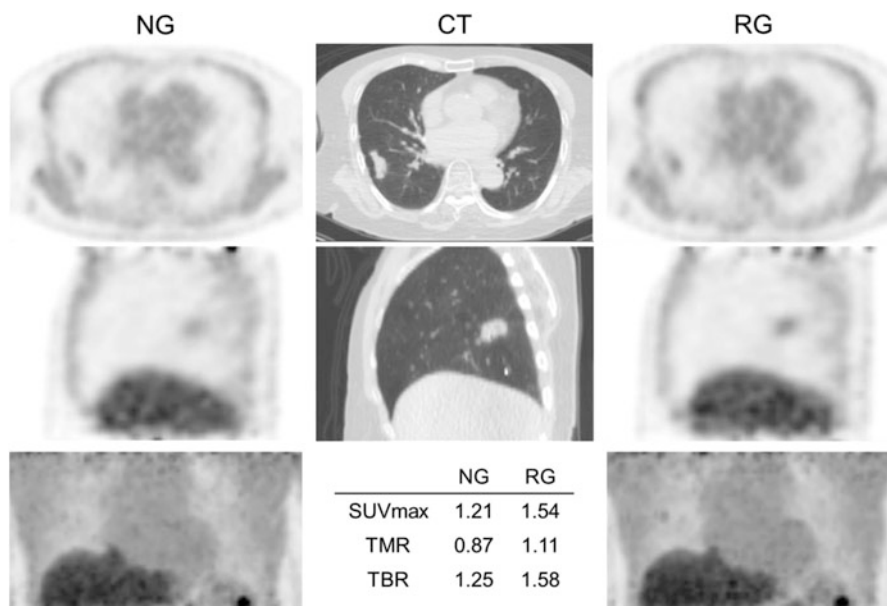


Fig. 25.4 Images of an 87-year-old female with stage II NSCLC in the right lower lobe. In non-respiratory-gated maximum intensity projection (MIP) imaging, no primary lesion was detected. However, in respiratory-gated MIP imaging, the lesion was visually detected

Table 25.2 SUVmax, TMR, and TBR of lesions on RG and NG images

	SUVmax		TMR		TBR	
	NG	RG	NG	RG	NG	RG
Mean	1.93	2.09	1.46	1.61	1.42	1.53
SD	1.11	1.11	0.78	0.78	0.87	0.86

Abbreviations: *NG* non-gating, *RG* respiratory gating, *SD* standard deviation, *SUVmax* maximum standardized uptake value, *TBR* tumor-to-blood ratio, *TMR* tumor-to-muscle ratio

reoxygenation in the former [9]. Information on tumor hypoxia may be used to modify the radiation planning, especially the treatment fraction, to maximize cytotoxic effects.

However, as mentioned above, respiratory motion during PET image quantification can introduce image misregistration errors, and if uncorrected images are acquired, such errors may eventually hinder adequate patient management [10]. As a combined treatment strategy with functional information provided by PET imaging, correction of PET images for respiratory motion artifacts may increase the efficacy of individually tailored therapy. If FMISO-PET imaging predicts local failure, then it can be used for guiding the selection of patients who would benefit from dose escalation, modification of fractionation, or additional treatment with a hypoxic cell radiosensitizer.

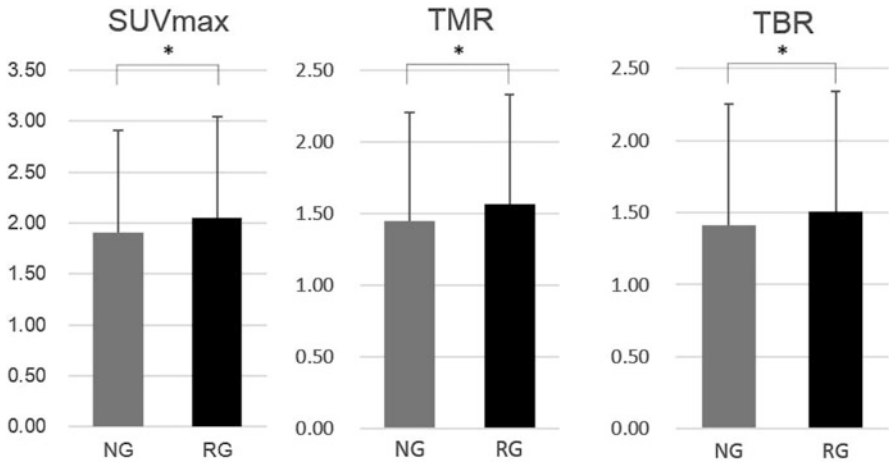


Fig. 25.5 SUVmax, TMR, and TBR were significantly higher on RG images than on NG images (* $p < 0.05$, paired t -test)

Table 25.3 Increase in HV with RG

Age	Sex	HV in NG	HV in RG
72	Male	0	0.19
50	Male	9.15	9.92
62	Female	52.54	53.12
85	Male	2.05	2.69
81	Male	0.00	0.13
Mean		12.8	13.2
SD		22.6	22.7

Abbreviations: *HV* hypoxic volume, *NG* non-gating, *RG* respiratory gating, *SD* standard deviation

One of the limitations of our study was the relatively small number of patients examined. Further clinical study will be required to clarify the diagnostic value of the quantitative evaluation of hypoxia with RG in association with local recurrence and prognosis.

25.4 Conclusion

Respiratory gating in FMISO-PET/CT could provide higher sensitivity of hypoxic evaluation and accurate quantification of hypoxia.

Open Access This chapter is distributed under the terms of the Creative Commons Attribution-Noncommercial 2.5 License (<http://creativecommons.org/licenses/by-nc/2.5/>) which permits any noncommercial use, distribution, and reproduction in any medium, provided the original author(s) and source are credited.

The images or other third party material in this chapter are included in the work's Creative Commons license, unless indicated otherwise in the credit line; if such material is not included in the work's Creative Commons license and the respective action is not permitted by statutory regulation, users will need to obtain permission from the license holder to duplicate, adapt or reproduce the material.

References

1. Yip C, Blower PJ, Goh V, Landau DB, Cook GJ. Molecular imaging of hypoxia in non-small-cell lung cancer. *Eur J Nucl Med Mol Imaging*. 2015;42(6):956–76. doi:[10.1007/s00259-015-3009-6](https://doi.org/10.1007/s00259-015-3009-6).
2. Gray LH, Conger AD, Ebert M, Hornsey S, Scott OC. The concentration of oxygen dissolved in tissues at the time of irradiation as a factor in radiotherapy. *Br J Radiol*. 1953;26(312):638–48. doi:[10.1259/0007-1285-26-312-638](https://doi.org/10.1259/0007-1285-26-312-638).
3. Gilkes DM, Semenza GL, Wirtz D. Hypoxia and the extracellular matrix: drivers of tumour metastasis. *Nat Rev Cancer*. 2014;14(6):430–9. doi:[10.1038/nrc3726](https://doi.org/10.1038/nrc3726).
4. Cherk MH, Foo SS, Poon AM, Knight SR, Murone C, Papenfuss AT, et al. Lack of correlation of hypoxic cell fraction and angiogenesis with glucose metabolic rate in non-small cell lung cancer assessed by 18F-Fluoromisonidazole and 18F-FDG PET. *J Nucl Med Off Publ Soc Nucl Med*. 2006;47(12):1921–6.
5. Callahan J, Kron T, Schneider-Kolsky M, Hicks RJ. The clinical significance and management of lesion motion due to respiration during PET/CT scanning. *Cancer Imaging Off Publ Int Cancer Imaging Soc*. 2011;11:224–36. doi:[10.1102/1470-7330.2011.0031](https://doi.org/10.1102/1470-7330.2011.0031).
6. Bettinardi V, Picchio M, Di Muzio N, Gilardi MC. Motion management in positron emission tomography/computed tomography for radiation treatment planning. *Semin Nucl Med*. 2012;42(5):289–307. doi:[10.1053/j.semnuclmed.2012.04.001](https://doi.org/10.1053/j.semnuclmed.2012.04.001).
7. Jani SS, Robinson CG, Dahlbom M, White BM, Thomas DH, Gaudio S, et al. A comparison of amplitude-based and phase-based positron emission tomography gating algorithms for segmentation of internal target volumes of tumors subject to respiratory motion. *Int J Radiat Oncol Biol Phys*. 2013;87(3):562–9. doi:[10.1016/j.ijrobp.2013.06.2042](https://doi.org/10.1016/j.ijrobp.2013.06.2042).
8. Okamoto S, Shiga T, Yasuda K, Ito YM, Magota K, Kasai K, et al. High reproducibility of tumor hypoxia evaluated by 18F-fluoromisonidazole PET for head and neck cancer. *J Nucl Med Off Publ Soc Nucl Med*. 2013;54(2):201–7. doi:[10.2967/jnumed.112.109330](https://doi.org/10.2967/jnumed.112.109330).
9. Meng X, Kong FM, Yu J. Implementation of hypoxia measurement into lung cancer therapy. *Lung Cancer (Amsterdam, Netherlands)*. 2012;75(2):146–50. doi:[10.1016/j.lungcan.2011.09.009](https://doi.org/10.1016/j.lungcan.2011.09.009).
10. Grootjans W, de Geus-Oei LF, Meeuwis AP, van der Vos CS, Gotthardt M, Oyen WJ, et al. Amplitude-based optimal respiratory gating in positron emission tomography in patients with primary lung cancer. *Eur Radiol*. 2014;24(12):3242–50. doi:[10.1007/s00330-014-3362-z](https://doi.org/10.1007/s00330-014-3362-z).